ELSEVIER

Contents lists available at ScienceDirect

Science of the Total Environment

journal homepage: www.elsevier.com/locate/scitotenv





Dryland ecosystem regeneration and plant metal(loid) accumulation strategies 60 years after revegetating a mine tailings pond

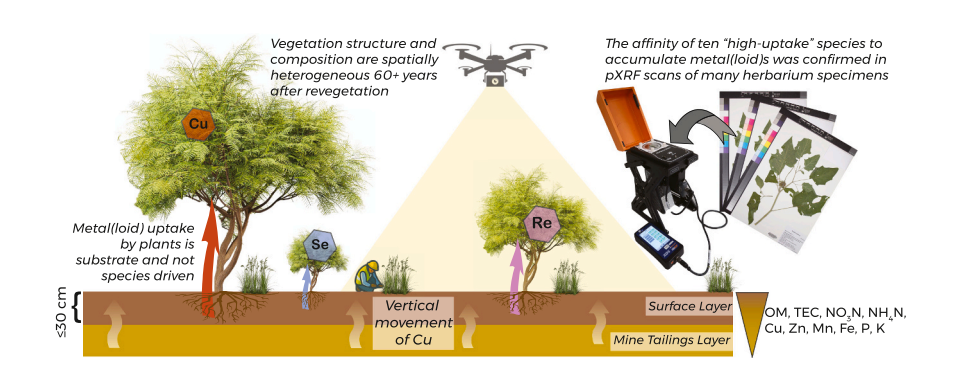
Tomasz Włodarczyk ^{a,*}, Flurin Babst ^{b,c}, Kamila Murawska-Włodarczyk ^a, Owyn Stokes ^a, Andrew Salywon ^d, Willem J.D. van Leeuwen ^{b,e}, Cynthia Libantino Norton ^b, Shelby Rader ^f, Raina M. Maier ^a, Alicja Babst-Kostecka ^{a,g}

- ^a Department of Environmental Science, The University of Arizona, Tucson, AZ, USA
- ^b School of Natural Resources and the Environment, The University of Arizona, Tucson, AZ, USA
- ^c Laboratory of Tree-Ring Research, The University of Arizona, Tucson, AZ, USA
- ^d Department of Research, Conservation and Collections, Desert Botanical Garden, AZ, USA
- ^e School of Geography, Development & Environment, The University of Arizona, Tucson, AZ, USA
- ^f Department of Earth and Atmospheric Sciences, Indiana University, Bloomington, IN, USA
- g Bio5 Institute, The University of Arizona, Tucson, AZ, USA

HIGHLIGHTS

- The plant community across an arid tailings pond remains heterogeneous after 60 years.
- Substrate properties and topsoil regeneration drive elemental uptake by plants.
- We discovered new (hyper)accumulators of Cu, Se, and Re in the U.S. Southwest.
- pXRF herbarium scans of candidate taxa for remediation confirm large-scale potential.

G R A P H I C A L A B S T R A C T



ARTICLE INFO

Keywords: Hyperaccumulators Metallophytes Phytoremediation Mining Herbarium XRF Remote sensing

ABSTRACT

The revegetation of anthropogenically degraded sites is challenging in drylands where the combination of harsh substrates and climatic stress creates a restrictive environment. Mine tailings are particularly complex, and the number of successfully revegetated sites has remained small. Our study aimed to investigate one of the few successfully revegetated Cu-Mo tailings ponds in a semi-arid part of the U.S. Southwest to improve our understanding of the drivers and barriers of plant establishment. Integrating in situ vegetation surveys, biochemical analyses of plants and soils, and remote sensing, we assessed vegetation structure, composition, and metal(loid) uptake in various sections of the tailings pond and an adjacent natural area. Based on a hierarchical cluster analysis, we found that plant communities at different successional stages corresponded to specific substrate properties across the site. Depending on the biochemistry and thickness of the surface soil, plants exhibited variable nutrients and metal(loid) accumulation in foliage. We also found that certain soil properties may facilitate the mobility of Cu from tailings layers to the surface. Intriguingly, some of the species (hyper)

^{*} Corresponding author at: The University of Arizona, Thomas W. Keating Bioresearch Bldg., 1657 E Helen St., 85721, USA. *E-mail address:* twlodarczyk@arizona.edu (T. Wlodarczyk).

accumulated Cu, Se, and Re at levels of up to \sim 750, \sim 80, and \sim 90 mg kg $^{-1}$ respectively. For these species, we established robust elemental benchmarks through the X-ray fluorescence screening of many herbarium specimens from uncontaminated natural locations and confirmed their affinity for elevated metal(loid) accumulation at a larger scale. Our findings can facilitate species selection for future reclamation research and applications. Upcoming work may leverage the same methodological framework to continue closing the knowledge gap of the factors that determine revegetation success or failure in drylands.

1. Introduction

Anthropogenic land degradation is a global issue, with approximately 33 % of the global land surface currently affected by land degradation and desertification. These processes, exacerbated by climate change and biodiversity loss, are closely linked to declining environmental health and ecosystem services (Raj et al., 2023). Hardrock mining contributes substantially to this land degradation and innovative science-based mitigation measures are urgently needed to help remediate mining-impacted lands (Sun et al., 2021). Creating a lasting vegetative cover is central to risk-based phytomanagement particularly phytostabilization - and is widely used to reclaim miningimpacted lands in dryland ecosystems (Mendez and Maier, 2008). The benefits of revegetation include: stabilization of mine sites against wind and water erosion; suppression of dust generation; restoration of carbon (C) sequestration capacity; facilitation of efficient evapotranspiration cap performance to contain acid generating and metal(loid) contaminated mine waste materials; restoration of visually pleasing landscapes; and environmentally responsible post-mining land use for securing the social license for future mining activities (Macdonald et al., 2015; Maiti and Ahirwal, 2019). Key factors like mine waste properties (e.g., low pH, salinity/sodicity, elevated metal(loid) concentrations), vegetation composition, and land management practices influence revegetation success (Mendez and Maier, 2008). In turn, a diverse and healthy plant community positively impacts the biophysicochemical properties of mine wastes, increasing litter accumulation, microbial biomass, and C, nitrogen (N), and phosphorus (P) content, as well as enhancing its water holding capacity (Singh et al., 2023). Ultimately, successful revegetation can create conditions that support key soil-based ecosystem functions comparable to those in nearby natural areas, regardless of the metal (loid) concentrations (Álvarez-Rogel et al., 2021).

The revegetation of mine sites is typically challenged by nutrient deficiencies, lack of soil structure, and a shortage of plant-growthpromoting soil microbes. Further, many legacy sites are characterized by low pH, high electrical conductivity (EC), and/or high metal(loid) content, which limits the number of viable plant species that can tolerate such conditions (Mendez and Maier, 2008). The release of excess metal (loid)s from mining operations stands out as a particularly severe threat to plants, animals, and microorganisms. However, certain plants called metallophytes have evolved mechanisms that allow them to tolerate and thrive in metalliferous ecosystems (Baker et al., 2010). These plants represent a key resource for ecological restoration and fall into three categories based on their strategies for managing potentially toxic metals: excluders, which restrict metal uptake and translocation to above-ground parts; indicators, where metal uptake and transport to shoots increase with soil metal concentrations; and accumulators, which uptake, translocate, and sequester high concentrations of metals in above-ground parts, often regardless of soil levels. Selecting appropriate metallophytes for revegetation of metal(loid)-contaminated sites is thus critical to controlling metal(loid) fate (Baker, 1981; Mendez and Maier, 2008). In drylands, excluder species are typically prioritized for phytostabilization, but assessing accumulator traits is also valuable: it identifies potential food-web risks, clarifies plant-soil feedbacks, and, in some cases, can inform the development of emerging phytoextraction or phytomining technologies (Rylott and Ent, 2025). Biomass quantification and post-harvest management are critical for the latter approaches to prevent secondary pollution. Plant surveys at successfully revegetated

post-industrial landscapes are thereby instrumental in identifying key metallophytes suitable for various phytomanagement strategies across different climatic regions.

To date, most studies on plant metallomes (the metal(loid) content in the plant) have been based on short-term assessments of vegetation established under varying climatic conditions. By contrast, datasets that assess established plant communities multiple decades post revegetation are rare but critical, as the recovery on mine wastes often requires multiple decades to stabilize key soil and vegetation functions (Tay et al., 2021). Such long-term information is needed for selecting suitable plant species for phytomanagement yet remains particularly limited in arid and semi-arid environments. These drylands can experience extreme temperatures, drought, and elevated soil salinity (Mendez and Maier, 2008) and overall rank among the least understood ecosystems in terms of adaptation to global change (Feldman et al., 2024). One particularly relevant dryland region is the U.S. Southwest, a biodiversity hotspot and leading provider of mineral commodities (USGS, 2024). In this area, revegetation is additionally challenged by a short growing season, pulse-driven precipitation, and low annual rainfall. These harsh conditions, combined with our insufficient understanding of droughtadapted metallophytes, have hampered the establishment of a selfsustaining and lasting ecosystem on many mining-impacted drylands (Mendez and Maier, 2008).

The growing demand for mineral resources and a legacy of over 160,000 abandoned mine sites in the western U.S. (Lewis et al., 2017) underscore the need to close the above-listed knowledge gaps and generate science-driven revegetation strategies. Here we present a multifaceted approach to survey dryland metallophytes on one of the few successfully revegetated tailings ponds in the U.S. Southwest, identify their individual metal(loid) uptake strategies, and study plantsubstrate interactions. First, we conducted a traditional field survey within tailing plots and on neighboring undisturbed land to assess the plant community composition and collect plant and substrate samples. The samples were analyzed in the laboratory to identify metal(loid) excluder, indicator, and accumulator species, and assess plant-driven improvements in substrate quality. Survey periods were limited to the early spring (February-April) and post-monsoon (July-September) seasons when it was possible to identify native annual plants with short life cycles that contribute significantly to plant diversity in the desert (Archer and Predick, 2008). Second, we conducted an airborne remote sensing campaign using drone Light Detection and Ranging (LiDAR) to assess the aboveground vegetation structure within the same plots. Third, the species identified as the most promising metal(loid) accumulators – which may find application in phytomining technologies – were further explored to evaluate whether elemental accumulation traits are species- or population-dependent. For this purpose, we used a powerful yet underutilized approach where a large number of existing herbarium specimens from multiple natural but geographically close locations were scanned to benchmark metal(loid) uptake patterns observed in tailings plants. This novel workflow importantly allows us to draw conclusions regarding the phytostabilization and phytoextraction potential of key species beyond the site itself.

Using this combined approach, we addressed the following key questions:

- 1) Which vegetation characteristics (structure and composition) and biophysicochemical properties of the substrate reflect advanced versus poor ecosystem recovery 60+ years after revegetation?
- 2) To what extent does the vegetation structure and composition within tailings plots differ from that of neighboring undisturbed land?
- 3) Do the species that are present at this successfully revegetated site exhibit different metal(loid) uptake strategies (exclusion, indication, accumulation)?
- 4) Is high metal(loid) uptake in certain species a site-specific or specieswide characteristic?

Finally, we discuss our findings in the context of phytomanagement in drylands, with a particular focus on enhanced plant metal uptake in key species. This aspect has remained understudied in traditional research geared at the phytostabilization of mine tailings but now gains traction under the global trend towards circular economies and the push to extend metal life cycles through the secondary extraction from legacy mine waste.

2. Methods

2.1. Site description and field campaign

The study was conducted at a reclaimed tailings pond in central Arizona, U.S.A. (specific location details are withheld due to the land-owner's policy). The site spans $\sim 1~{\rm km}^2$ and was used for the disposal of Cu and molybdenum (Mo) sulfide-bearing mine tailings between 1928 and 1959. After the facility's closure, the surface was regraded, capped with a thin (15 cm) layer of locally sourced soil, and revegetated in 1960

using native seed mixes representative of the regional vegetation, without any soil amendments. A stable and self-sustaining plant community has since established and continued to thrive at the time of this study. The region experiences a semiarid climate, with an average annual precipitation of 397 mm and means annual temperature of 17.6 °C (United States National Weather Service, n.d.).

To support the selection of representative plots, we first acquired aerial imagery of the entire site and surrounding regions using a DJI Matrice 300 RTK drone equipped with an FPV RGB camera and LiDAR, providing an overview of vegetation distribution and structural variation (see Supplementary Materials for remote sensing methods). Briefly, image processing and spatial analyses were performed in ArcGIS Pro, DJI Terra, and R to generate an orthomosaic, create a digital surface model, and derive a canopy-height model. We then used a supervised classification based on spectral signature to categorize the orthomosaic into three classes: vegetation; vegetated soil (grasses and small forbs); and bare soil (non-vegetated soil and rocks). Guided by this data and field scouting, we delineated four study plots within the tailings pond (P1, P2, P3, P4; Fig. 1) chosen to represent variation in vegetation structure, composition, and coverage across the site. Plots were selected on flat areas between the check berms, constructed to divert excess stormwater through a spillway. Plots P1 (130 \times 90 m), P2 (200 \times 58.5 m), and P3 (130 \times 90 m) each averaged 11,700 m² in size whereas plot P4 covered a small and unique area (~1300 m²) of largely exposed bare soil and tailings. An extensive in-situ plant collection was conducted in early fall 2022 and spring 2023 to capture data after the monsoon and winter precipitation. Additionally, species matching those found at the tailings pond were collected from an undisturbed natural plot (~11,700 m^2 ; 130 × 90 m) on the northwestern side of the tailings pond (Fig. 1).

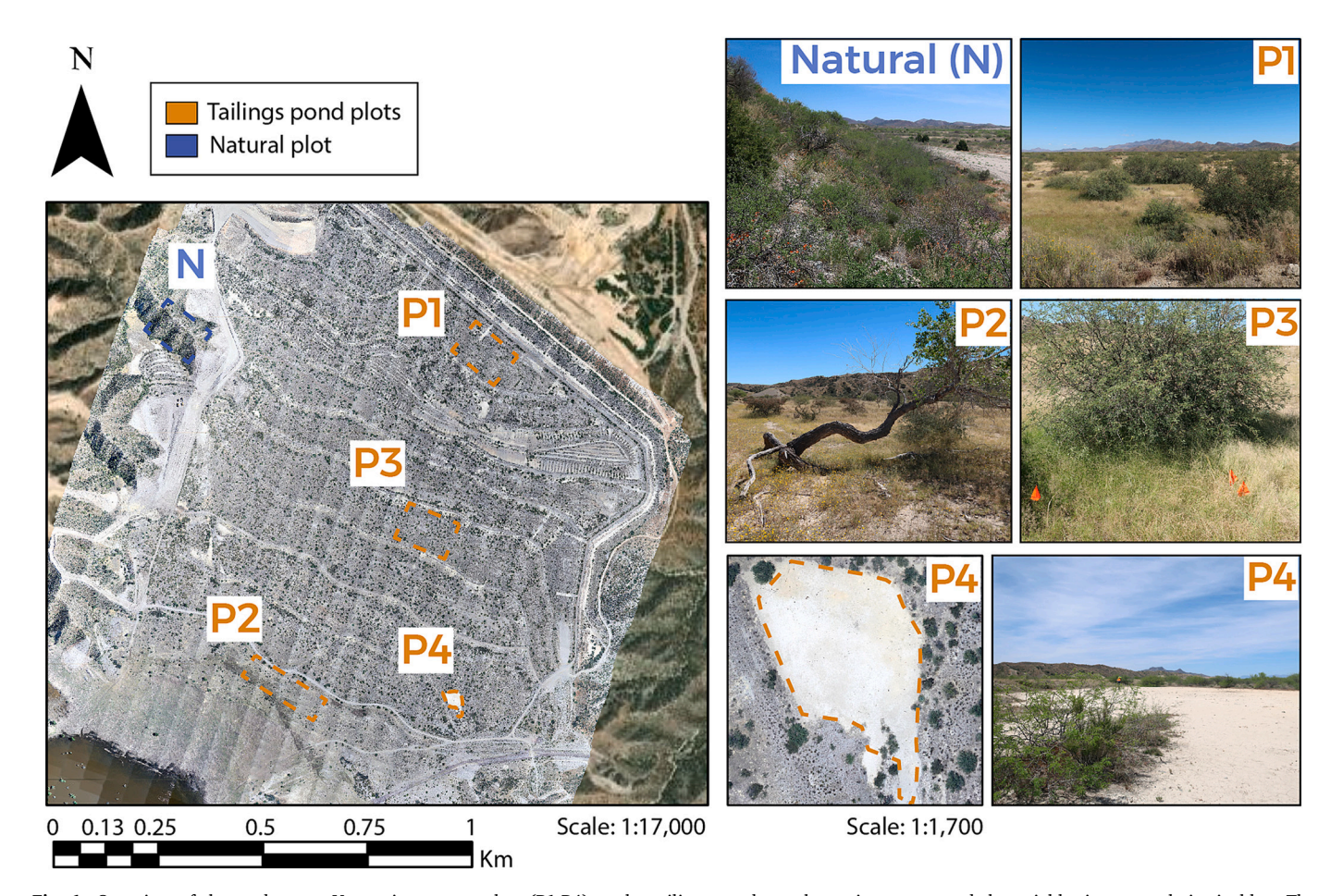


Fig. 1. Overview of the study area. Vegetation survey plots (P1:P4) at the tailings pond are shown in orange, and the neighboring natural site in blue. The orthomosaic was generated from images captured by an unmanned aerial vehicle (UAV) flight.

While no substantial elevation changes were observed within or near the selected plots, the natural site was steep and rocky, with an elevation up to 60 m higher than the tailings plots (Supplementary Fig. S1). Within each plot, the aboveground biomass of every present plant species was collected in up to six randomly selected replicates. Smaller plants were sampled as entire individuals, whereas multiple foliage samples were collected and combined from larger shrubs and trees. Each sample was wrapped in a moist paper towel, placed in a plastic bag, and stored in a cooler until transported to the lab. A total of 249 plant samples were collected from both tailings and natural plots. Each species was identified and linked to the corresponding voucher ID by the University of Arizona Herbarium. Soil samples (~400 g; nine from each tailing plot, five from the neighboring natural site) were collected in a grid pattern from the surface (if present; top \sim 30 cm) and from the underlying tailings layer (below ~30 cm depth). Additional soil samples (~7 g) were collected at each plot using sterile tools, placed into sterile tubes, and transported on dry ice to the lab and stored at -80 °C until processing for soil DNA quantification.

2.2. ICP-MS analyses of plant leaves

Plant samples (n = 249) were washed (2 \times 10 s in deionized and 1 \times 10 s in Milli-Q water) and air-dried. Then, leaves were separated from stems and oven-dried at 70 °C for 72 h. After drying, samples were transferred to a vacuum desiccator filled with silica gel. To mitigate impurities linked to commonly used grinding materials and ensure optimal mechanical tissue homogenization, leaf samples were packed into 4.5 mL tubes with two ceramic spheres (TallPrep Lysing Matrix M, 4.5 mL tube; MP Biomedicals, USA) and ground to fine powder (<1 mm) using a FastPrep-24 5G homogenizer (MP Biomedicals, USA).

Homogenized samples (≤500 mg) were microwave digested following (Stegink and Rader, 2024). Each digestion batch included certified reference materials (NIST 1547 Peach Leaves) and procedural blanks (see Supplementary Table S1 for NIST results). Digested samples were evaporated on a hot plate (90 °C) and redissolved in a 2 % HNO₃ solution. The concentrations of P, S, Fe, B, Mn, Zn, Cu, Mo, Ni, Be, Al, Si, Ti, V, Cr, Co, Ge, As, Se, Zr, Nb, Ag, Cd, Sb, Ba, Ta, W, Re, and Pb were measured using an Agilent 7850 Inductively Coupled Plasma Mass Spectrometry (ICP-MS; Santa Clara, CA), with each sample analysis consisting of the average of five blocks with 100 sweeps each. Elements were selected to capture essential plant nutrients (e.g., P, S, Fe, B, Mn, Zn, Cu, Mo), potential toxic metal(loid)s common in mining environments (e.g., Ni, Cr, Co, As, Cd, Pb), and lithogenic elements (e.g., Al, Si, Ti, Zr, Ba). Selenium and Re were specifically included based on our preliminary data indicating their uptake by dryland plants in this region. The ICP-MS analyses were conducted in the Metal Isotopes Laboratory at Indiana University, Bloomington, at the Department of Earth and Atmospheric Sciences.

2.3. ICP-MS analyses of soil and tailings samples and soil microbial biomass analysis

Soil and tailings samples (n = 76) were sieved (2 mm), ground, ovendried at 105–110 °C, and kept in a desiccator prior to weighing. For each sample, 0.1 g of material was pre-digested at room temperature in 1 mL concentrated HNO3 (Omni-trace HNO3, EMD Chemicals), followed by the addition of 1 mL ultrapure water (18 Ω). After the $\rm H_2O_2$ reaction subsided, the vessels were capped, soil samples were microwave digested (CEM Model MARS6 microwave, Matthews, North Carolina), and total concentrations of P, S, Fe, Mn, Zn, Cu, Mo, Ni, Al, Si, Se, and Re were analyzed with Agilent 7700x ICP-MS (Santa Clara, CA). Acid blanks and a certified reference material (NIST 2711 Montana soil) were included in each batch for quality assurance (see Table S1 for NIST results). Analyses were conducted by the University of Arizona Laboratory for Emerging Contaminants. Additionally, analyses of Mehlich III-extractable elements (P, S, Fe, Mn, Zn, Cu, Ca, K, Mg, Na), organic

matter (OM), total exchange capacity (TEC), pH, estimated N release (ENR), 1:2 soil-to-water EC, nitrate-N (NO $_3$ -N), and ammonium-N (NH $_4$ -N) were conducted by a commercial laboratory (Brookside Laboratories, New Bremen, Ohio; S005 soil analysis package, blinc.com).

Soil DNA was extracted from 0.25 g of soil (n = 33), using the DNeasy PowerLyzer PowerSoil kit (QIAGEN), and following the manufacturer's guidelines. Negative control samples (blanks), composed solely of reagents, were incorporated. The quantification of the total DNA content was conducted with a Qubit 2.0 Fluorometer and a high-sensitivity dsDNA assay kit (Invitrogen, Carlsbad, California, USA). Soil DNA concentration (expressed as ng $\rm g^{-1}$ of dry soil) was calculated factoring in the soil moisture content pertinent to each sample.

2.4. Herbarium X-ray Fluorescence (XRF) scanning

For 10 metal(loid)-accumulating plant species identified in this study, we selected 50 herbarium specimens per species from the University of Arizona and Desert Botanical Garden Herbaria utilizing loose foliage pieces. Each specimen represented a distinct non-mining sampling location and underwent elemental analysis. Total concentrations of Cu, Se, Re, Zn, Mn, Fe, P, S were quantified to assess natural variation in elemental accumulation and infer species-specific metal(loid) uptake strategies. Foliage tissue samples were measured in triplicate with an HD Rocksand portable X-ray Fluorescence analyzer (pXRF; XOS Inc., HDXRF®, USA). This analyzer utilizes a miniature X-ray tube (25-50 kV, $200 \,\mu\text{A}$) with a 25 mm Silicon Drift Detector, employing a double-curved crystal and focused monochromatic excitation beams in three energy regions to enhance the signal-to-noise ratio. To minimize background noise, the pXRF was mounted on a stand, and each sample was prepared by stacking at least two leaves and placing them directly on the illuminating window (Supplementary Fig. S2). To prevent crosscontamination, 12 µm X-Ray polypropylene films (X-Ray Optical Systems, Inc., USA) were exchanged between each sample. All samples were analyzed using T1.5 quantification mode for 90 s (30 s for each energy level) and the Plant optimization. To ensure quality assurance and control (QA/QC) during pXRF scanning, two certified reference materials (NIST 1573a and NIST 1570) were routinely analyzed together with a sucrose blank sample included every 20 measurements. The mean recovery values [(pXRF value/reference value) * 100] were calculated for NIST 1573a, NIST 1570, NIST 1515, NIST 1547, NIST 1568b, NIST 1575a, and two internal Re and Se reference samples: P (151 %), S (106 %), Fe (104 %), Mn (105 %), Zn (107 %), Cu (112 %), Se (109 %), Re (96 %), K (114 %), Ca (119 %). Note that P concentration should be interpreted with caution due to the high percent recovery and the element's susceptibility to air-path attenuation and interference from the polypropylene film (Towett et al., 2016).

2.5. Data processing and statistical analysis

Prior to plant, herbarium, and soil data analysis, non-detected values were substituted with half of the instrument's detection value for the respective parameter (USEPA, 2006). Outliers were removed from soil data using the interquartile range method (1.5 x IQR). Plant and soil datasets were verified for the residual normality with Quantile-Quantile, density plots and Shapiro-Wilk tests. Equality of variances between analyzed groups (substrate layers: surface vs. tailings; plots: P1-P4; and clusters revealed by hierarchical clustering) was assessed using Bartlett's and Levene's test. The best normalizing transformation functions were identified and applied when needed, using the bestNormalize package in R (Peterson, 2021). For parameters that met the assumptions for parametric tests, one-way ANOVA, followed by Tukey HSD post-hoc pairwise comparisons and student t-test were used. When assumptions remained unmet after transformation, non-parametric tests, including Kruskal-Wallis test, Dunn's multiple comparisons test, and Wilcoxon tests, were conducted. Soil data was standardized and further analyzed using hierarchical clustering with the "Ward.D2" method. All measured

Science of the Total Environment 1004 (2025) 1807

Table 1
Substrate biochemistry (mean \pm SD) from the natural site (n = 5) and tailings pond plots (n = 9 per plot). Data shown for both surface and tailings layers across four plots (P1:P4). Letters denote significant difference at $p \le 0.05$; ns – not significant; EC – electrical conductivity; OM – organic matter; ENR – estimated N release; TEC – total exchange capacity; ext. in the subscript indicates extractable fraction (Mehlich III) of the given element.

		Natural site	Tailings site							
			Plot P1		Plot P2		Plot P3		Plot P4	
			Surface	Tailings	Surface	Tailings	Surface	Tailings	Surface	Tailings
pН	_	7.9 ± 0.7^a	8.2 ± 0.2^{a}	8.0 ± 0.4^{a}	7.3 ± 0.8^{ab}	7.0 ± 1.1^{ab}	7.8 ± 0.3^{ab}	$8.1\pm0.2^{\rm a}$	6.4 ± 1.1^{bc}	$5.3\pm0.9^{\rm c}$
EC	mmhos/cm	0.30 ± 0.03^a	0.2 ± 0.1^{ab}	0.2 ± 0.1^{ab}	$0.10\pm0.05^{\mathrm{bc}}$	0.06 ± 0.01^{d}	0.20 ± 0.05^{ab}	$0.07\pm0.03^{\rm d}$	$0.10\pm0.06^{\rm b}$	0.07 ± 0.01^{cd}
OM	%	1.5 ± 0.1^{ab}	0.9 ± 0.1^{cd}	0.60 ± 0.04^{ce}	$1.1\pm0.3^{ m bd}$	$0.5\pm0.1^{\mathrm{e}}$	1.6 ± 0.3^{a}	$0.5\pm0.1^{\rm e}$	$0.9 \pm 0.3^{\mathrm{cd}}$	$0.5\pm0.1^{\rm e}$
ENR	N/acre	51 ± 1^{ab}	35 ± 4^{c}	24 ± 2^{d}	$40\pm8^{\mathrm{bc}}$	$19\pm5^{\rm d}$	53 ± 7^a	$19\pm5^{\rm d}$	34 ± 8^{c}	18 ± 6^{d}
TEC	meq/100 g	36 ± 6^a	21 ± 3^{abc}	14 ± 5^{bcd}	13 ± 4^{bcde}	$4.9\pm1.1^{\rm f}$	23 ± 6^{ab}	$6.8\pm4.3^{\rm ef}$	$12\pm8^{ m cde}$	$7.7 \pm 4.0^{\mathrm{def}}$
NO ₃ -N	${\rm mg~kg^{-1}}$	3.3 ± 2.0^a	2 ± 1^{ab}	$1.2\pm0.8^{\rm bc}$	2.9 ± 1.4^{a}	$0.6\pm0.3^{\rm c}$	3.2 ± 1.5^a	1.4 ± 0.3^{ab}	2.3 ± 0.6^{ab}	$1.0\pm0.5^{\rm bc}$
NH ₄ -N	$mg kg^{-1}$	1.4 ± 0.2^{bcd}	$1.2\pm0.3^{\rm bc}$	1.0 ± 0.2^{ac}	$1.3\pm0.3^{\rm bd}$	$0.9\pm0.2^{\rm c}$	2.2 ± 0.2^a	$1.5\pm0.1^{\rm b}$	2.2 ± 0.3^a	$0.9\pm0.2^{\rm c}$
Soil DNA	ng g ⁻¹	3.2 ± 0.3^a	$0.9 \pm 0.3^{\mathrm{cd}}$	$1.5\pm0.4^{\mathrm{bc}}$	$0.10\pm0.03^{\rm e}$	$0.6\pm0.4^{ m d}$	$1.3\pm0.8^{\mathrm{bd}}$	$1.7\pm0.7^{\mathrm{b}}$	$0.6\pm0.2^{\rm d}$	0.03_{2}^{f}
Cu	$mg kg^{-1}$	$262\pm51^{\rm d}$	1095 ± 179^{ab}	1756 ± 353^a	666 ± 147^{bcd}	$319\pm140^{\rm d}$	921 ± 340^{abc}	$275\pm93^{\rm d}$	1627 ± 958^{ab}	372 ± 111^{cd}
Se	$mg kg^{-1}$	1.1 ± 1.0^{ns}	1.1 ± 0.7^{ns}	2.0 ± 0.5^{ns}	0.8 ± 0.5^{ns}	$1.8\pm0.7^{\text{ns}}$	1.0 ± 0.8^{ns}	1.7 ± 0.8^{ns}	2.1 ± 1.3^{ns}	$1.9\pm0.8^{\text{ns}}$
Re	${\rm mg~kg^{-1}}$	0.002 ± 0.001^{b}	0.005 ± 0.002^{b}	0.010 ± 0.003^a	$0.005 \pm 0.002^{\rm b}$	$0.004 \pm 0.001^{\rm b}$	0.006 ± 0.004^{ab}	0.004 ± 0.001^{b}	0.010 ± 0.004^a	0.004 ± 0.001^{b}
Zn	${\rm mg~kg^{-1}}$	50 ± 5^{ab}	$33\pm3^{\mathrm{bc}}$	19 ± 4^{c}	$32\pm12^{\rm bc}$	$7.8\pm1.1^{\rm d}$	61 ± 13^{a}	$7.4\pm2.1^{\rm d}$	$28\pm12^{\rm c}$	$8.6\pm2.7^{\rm d}$
Mn	${\rm mg~kg^{-1}}$	306 ± 38^a	190 ± 14^{bc}	$113\pm46^{\rm c}$	147 ± 42^{c}	48 ± 9^{d}	267 ± 37^{ab}	44 ± 2^{d}	97 ± 29^{c}	42 ± 12^{d}
Fe	${\rm mg~kg^{-1}}$	$16,414 \pm 1628^a$	$8721\pm778^{\mathrm{bc}}$	7522 ± 1052^{cd}	8468 ± 1144^{bc}	$6529 \pm 482^{\mathrm{de}}$	$12{,}404 \pm 2982^{ab}$	$6309 \pm 891^{\rm e}$	7601 ± 1427^{ce}	$6483 \pm 537^{\text{de}}$
Al	mg kg ⁻¹	$15,217 \pm 2158^a$	$5921 \pm 1230^{\mathrm{b}}$	3068 ± 1385^{c}	5556 ± 1323^{b}	$2414 \pm 515^{\mathrm{c}}$	$12,627 \pm 3731^a$	2672 ± 839^{c}	5957 ± 1587^{b}	2493 ± 354^{c}
Mo	mg kg ⁻¹	$0.9\pm0.4^{\rm f}$	$4.8\pm0.9^{\rm ef}$	$9.7\pm2.0^{ m cd}$	$7.2\pm2.3^{\rm de}$	14 ± 4^{bc}	$5.3\pm3.0^{\rm ef}$	$9.0\pm1.7^{ m de}$	19 ± 1^a	16 ± 4^{ab}
Si	mg kg ⁻¹	2569 ± 208^a	285 ± 88^{cd}	$156\pm13^{\rm e}$	$206\pm31^{\rm de}$	$167\pm38^{\rm e}$	256 ± 87^{cd}	$580\pm560^{\rm d}$	2070 ± 524^{ab}	$1189 \pm 456^{\mathrm{bc}}$
Ni	mg kg ⁻¹	23 ± 3^a	$14\pm2^{\mathrm{b}}$	$8.9\pm2.8^{\rm c}$	10 ± 1^{c}	$5.3\pm1.1^{\rm d}$	20 ± 3^a	$5.1\pm1.1^{\rm d}$	$9.7\pm2.6^{\rm c}$	5 ± 1^d
P	${\rm mg~kg^{-1}}$	646 ± 40^a	515 ± 132^{ab}	243 ± 81^{cd}	405 ± 102^{ab}	$191\pm15^{\rm c}$	561 ± 101^{ab}	$219 \pm 31^{\rm cd}$	323 ± 55^{bd}	212 ± 18^{cd}
S	${\rm mg~kg^{-1}}$	$130\pm30^{\rm e}$	584 ± 248^{ab}	798 ± 187^a	532 ± 235^{abc}	340 ± 154^{bcde}	404 ± 199^{bcd}	501 ± 140^{abc}	287 ± 21^{cde}	$226\pm114^{\text{de}}$
Cu _{ext}	${\rm mg~kg^{-1}}$	100 ± 62^{e}	330 ± 28^{ab}	801 ± 255^a	266 ± 35^{bc}	$113\pm53^{\rm e}$	$222\pm139^{\mathrm{be}}$	$133 \pm 61^{\text{de}}$	789 ± 450^{ac}	322 ± 115^{bc}
Zn _{ext}	mg kg ⁻¹	$0.9\pm0.7^{\mathrm{bc}}$	1.7 ± 0.3^{ab}	2.5 ± 0.6^a	2.2 ± 0.3^a	$0.6\pm0.2^{\mathrm{c}}$	2.7 ± 0.9^a	0.4 ± 0.2^{c}	$3.0\pm1.3^{\text{a}}$	$1.2\pm0.3^{\rm bc}$
Mn_{ext}	${\rm mg~kg^{-1}}$	40 ± 13^{ab}	26 ± 12^{bc}	$6.1\pm1.8^{ m fg}$	18 ± 7^{bd}	$6.9 \pm 1.9^{ ext{efg}}$	48 ± 11^a	$5.5\pm1.9^{\rm f}$	12 ± 5^{cde}	$8.2\pm1.7^{\rm dg}$
Fe_{ext}	mg kg ⁻¹	29 ± 18^{d}	154 ± 17^{cd}	388 ± 106^{ab}	272 ± 81^{abc}	233 ± 80^{bc}	$52\pm19^{ m d}$	252 ± 98^{bc}	230 ± 96^{bc}	430 ± 88^a
S_{ext}	${\rm mg~kg^{-1}}$	$13\pm1^{ m abc}$	$10 \pm 2^{\mathrm{bcd}}$	34 ± 21^a	$11\pm2^{\mathrm{bcd}}$	$9.9 \pm 3.1^{\mathrm{bcd}}$	$8.7\pm1.4^{\rm cd}$	$6.6\pm2.2^{\rm d}$	17 ± 10^{abc}	22 ± 9^{ab}
P _{ext}	${\rm mg~kg^{-1}}$	20 ± 1^{abc}	14 ± 2^{bc}	5.8 ± 0.7^{c}	29 ± 4^a	20 ± 5^{ab}	27 ± 5^a	20 ± 7^{ab}	25 ± 11^a	30 ± 3^a
Ca _{ext}	${ m mg~kg^{-1}}$	7088 ± 637^a	3744 ± 573^{b}	2469 ± 890^{c}	1873 ± 498^{c}	702 ± 203^{de}	4104 ± 1089^b	976 ± 325^{df}	$1164 \pm 415^{\rm f}$	523 ± 100^e
K _{ext}	${\rm mg~kg^{-1}}$	125 ± 27^{bc}	111 ± 16^{bc}	53 ± 14^{cd}	96 ± 24^c	40 ± 7^{cd}	172 ± 34^a	35 ± 7^{d}	134 ± 39^{ab}	58 ± 7^{c}
Mg _{ext}	${\rm mg~kg^{-1}}$	140 ± 40^{ab}	124 ± 26^{ab}	87 ± 22^{bc}	172 ± 48^a	58 ± 4^{cd}	166 ± 11^a	35 ± 7^{d}	126 ± 34^{ab}	56 ± 9^{cd}
Na _{ext}	mg kg ⁻¹	17 ± 3^{ab}	17 ± 2^{ab}	$15\pm2^{\mathrm{bc}}$	35 ± 5^a	17 ± 1^{ab}	15 ± 1^{bc}	12 ^c	14 ± 2^{bc}	15 ± 1^{bc}

¹ All samples with the same value recorded (SD = 0).

² Single sample with quantifiable soil DNA biomass.

soil parameters were used in soil clustering. These included elements relevant to plant health and toxicity (P, S, Fe, Mn, Zn, Cu, and Mo), indicators of substrate lithology (Si, Al), and other commonly assessed biophysicochemical parameters (OM, TEC, pH, ENR, EC, NO_3 -N, and NH_4 -N).

For plant data, total metal(loid) concentrations were averaged by species at the plot level and normalized for heatmap visualization. The same hierarchical clustering method as in the soil analyses was applied. To explain variations in concentrations of Cu, Se, Re, Zn, Mn, Fe, P, S in plant leaves, Partial Least Squares Regression (PLS-R) models were developed. Each plant element was modeled individually as the dependent variable, with 30 soil parameters included as quantitative predictors and five plots as qualitative variables. The number of descriptors was optimized using the leave-some-out method (Roy and Roy, 2008) and a Jackknife cross-validation method with automatic stop conditions criteria. PLS-R models were developed in XLSTAT (Lumivero). All other statistical analyses and visualizations were performed in the R environment (version 4.2.2, R Core Team, 2022) .

3. Results

3.1. Site characteristics and substrate properties

The thickness of the capping soil layers differed notably between the study plots. Plot P3 had the thickest layer (up to 30 cm), followed by P1 and P2 (\sim 20 cm), while P4 had the thinnest layer (<10 cm), with some areas lacking the cap layer entirely.

The substrate characteristics of the natural plot and the plots located on the tailings pond differed substantially, with the latter exhibiting notable heterogeneity as indicated by high coefficient of variation values for multiple parameters (Table 1, Supplementary Table S2). Substrate pH ranged from neutral to moderately alkaline (7.0 to 8.2) at both natural and tailings locations, except for the P4 plot where acidic conditions prevailed; EC remained low across all locations (<0.3 mmhos cm⁻¹), indicating non-saline conditions. Organic matter content averaged ~ 1.3 % at both the natural site and the surface layer of the tailings pond, but was about 50 % lower in the underlying tailings layer. Total exchange capacity ranged from 36 meq/100 g at the natural site to 8 meq/100 g in the tailings layer of the tailings pond. Soil microbial DNA concentrations were several times higher at the natural site compared to the tailings pond. The latter also had significantly higher concentrations of total Cu, Re, Mo, S, and extractable Cu, Zn and Fe, while total Mn, Fe, Si, Ni, P, and extractable Mn and Ca were significantly lower than at the natural site (Supplementary Table S2), where Cu concentrations remained within the normal range for unpolluted soils (Chesworth et al., 2008). By contrast, the tailings pond substrate exceeded the Cu thresholds but remained below Arizona's remediation limits (Hard et al., 2019). Overall, the tailings layer consistently showed lower values for most elements compared to the surface and natural site, except for total

Mo and extractable Fe that were significantly higher.

Regarding the variability across plots, plot P3 stood out, with its surface layer exhibiting the highest levels of soil microbial DNA, OM, ENR, TEC, NO₃-N, total Zn, Mn, Fe, Al, Ni, P, extractable Mn, P, Ca and K. It also had the lowest concentrations of extractable Fe and S compared to the other plots. In contrast, the surface layer of P4 had the most distinct characteristics, including the highest mean concentrations of total Mo, Si, and extractable Cu, Zn, and S, alongside the lowest extractable Mn, Ca, TEC, and slightly acidic pH in both layers.

Cluster analysis of all substrate samples from natural and tailings pond sites identified four main groups of samples: (1) Substrate Group 1 included samples from the natural site and the surface layer of P3; (2) Substrate Group 2 comprised surface layers of P1 and P2; (3) Substrate Group 3 consisted of the surface layer of P4 and the tailings layer of P1; and (4) Substrate Group 4 included the tailings layers of P2, P3, and P4 (Fig. 2). This analysis further highlighted that conditions at P3 were closest to those found at the natural site, as well as the unique properties of the surface layer of P4. Overall, a significant decrease in EC, OM, ENR, TEC, total Zn, Mn, Fe, Al, Ni, and extractable Mn, Ca, K and Mg was observed across the substrate groups (Substrate Group 1 > Substrate Group 2 > Substrate Group 3 > Substrate Group 4), likely driving this classification (Fig. 3). Substrate Group 3 exhibited higher concentrations of total Cu, Re, and extractable S, Cu, and Zn compared to the other groups. A distinctive feature of Substrate Group 2 was its elevated concentrations of extractable Na.

3.2. Vegetation status and plant elemental variability

Overall, 40 plant species from 20 plant families were identified at the studied reclaimed tailings pond. These species represented eight grasses. 15 forbs, eight shrubs, and eight trees. The majority (~70 %) were perennial and native to Arizona, with four species classified as invasive. The list of all plant species with their botanical names, common names, family names, and voucher IDs is provided in the Supplementary Table S3. Species occurrence specific to each plot is shown in Fig. 4. Species richness was highest at plot P1 (24 species), followed by P2 (22), P3 (20), and P4 (12). Only ten species from the tailings pond overlapped with those from the neighboring natural site, including Allionia incarnata L., Berberis haematocarpa Wooton, Boechera perennans (S.Watson) W.A. Weber, Ceanothus greggii A. gray, Euphorbia melanadenia Torr., Gutierrezia sarothrae (Pursh) Britton & Rusby, Juniperus arizonica (R.P. Adams) R.P. Adams, Mimosa biuncifera Benth, Senegalia greggii (A. Gray) Britton & Rose (syn. Acacia greggii A. Gray), and Sphaeralcea parvifolia A. Nelson (Fig. 4, Table 2). Among the tailings pond plots, P3 shared the highest number (eight) of overlapping species with the natural site. P4 had the sparsest vegetation, with plants clustered in scattered clumps. This was likely due to the lack of a surface soil layer, resulting in exposed tailings.

Elemental analysis of field-collected plants revealed elevated concentrations of Cu, Se, and Re at the tailings plots (Supplementary Table

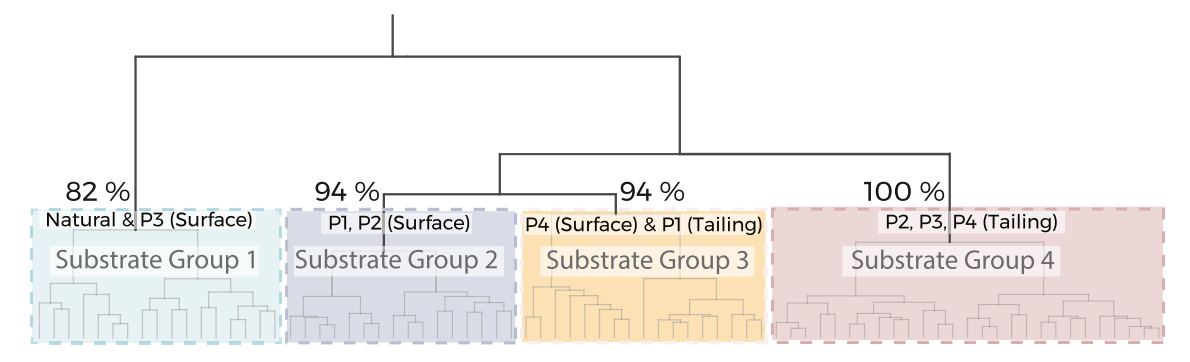


Fig. 2. Hierarchical clustering of substrate samples from the reclaimed tailings pond and a neighboring natural site. Clusters are based on 30 different soil parameters and correspond to different plots (P1, P2, P3, P4) and substrate layers (surface soil; tailings). The percentage of samples assigned to each cluster that originated from the listed sampling location is shown for each cluster, indicating good separation and compactness corresponding to sample origin.

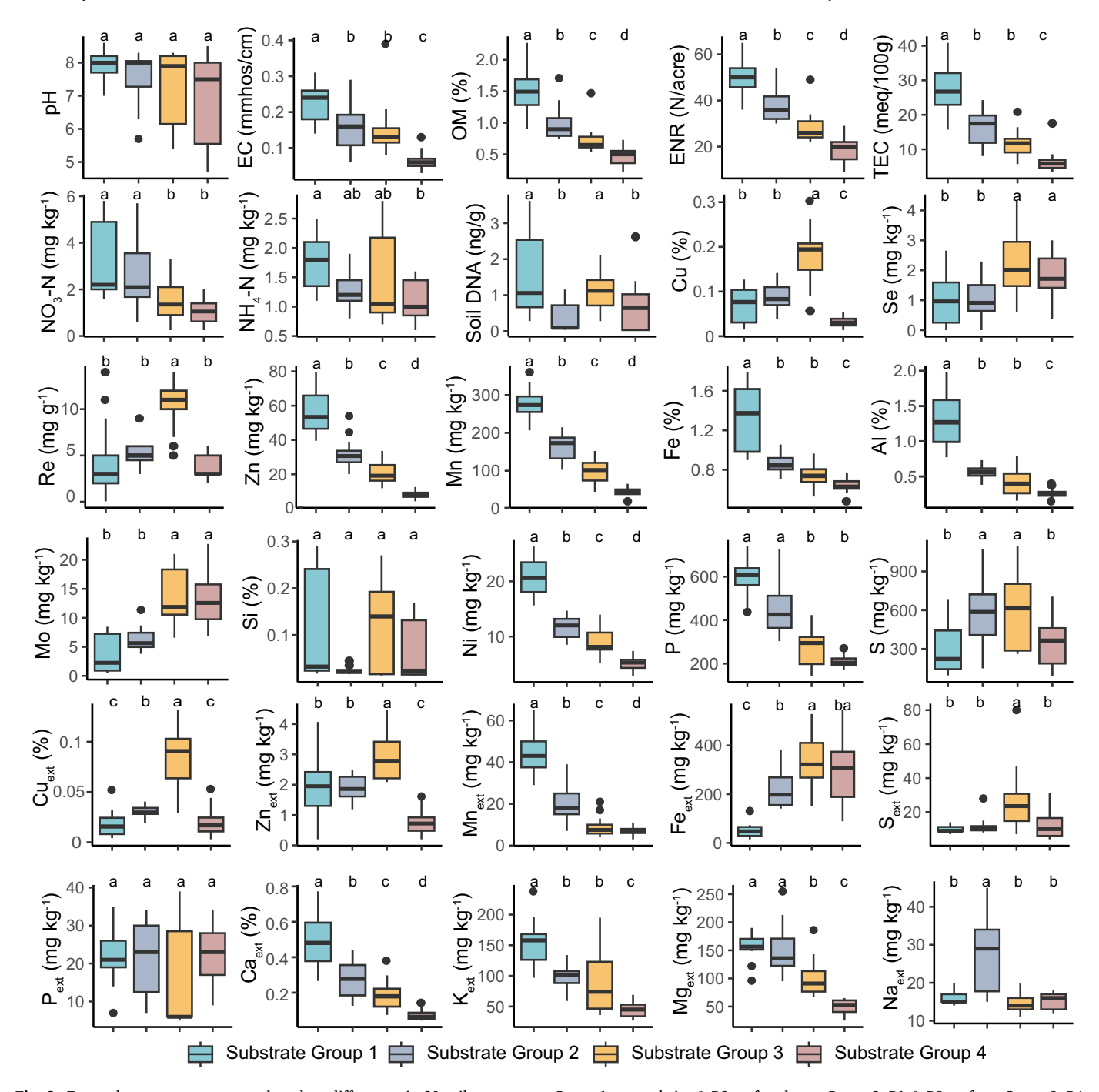


Fig. 3. Four substrate groups emerge based on differences in 30 soil parameters. Group 1: natural site & P3 surface layer; Group 2: P1 & P2 surface, Group 3: P4 surface & P1 tailings, Group 4: P2, P3 & P4 tailings. The box represents the 25th and 75th percentiles of the data, the median is indicated by the horizontal line. Letters denote significant difference between distributions; EC – electrical conductivity; OM – organic matter; ENR – estimated N release; TEC – total exchange capacity; ext. - extractable fraction (Mehlich III) of the given element.

S4). To better understand these uptake patterns and their ecological significance, they were further analyzed in conjunction with essential micro- and macronutrient concentrations in plant leaves, including Zn, Mn, Fe P, and S. A plant cluster map was created to capture similarities in elemental uptake across different families, genera, species, functional types, plot, and associations with the four main substrate clusters shown in Fig. 2. Three distinct plant groups were identified in this analysis (Fig. 5). Plant Group 1 exhibited the lowest concentrations of most elements, except for Zn, which remained consistent across all groups. This group had the highest proportion of grasses from the *Poaceae* family and annual plants. Plant Group 2 showed moderate elemental uptake and

consisted of a diverse mix of species spanning various functional types and families. This group included the highest number of species collected at locations that corresponded to Substrate Group 1 (i.e., the natural site and the surface layer of P3). In contrast, Plant Group 3 was characterized by the highest relative uptake of elements, with significantly higher concentrations of Cu and Mn. This group included many forbs and tree species (but no grasses) collected from plot P4, the surface of which was associated with Substrate Group 3. Within this group, 10 species present at the revegetated tailings pond were identified as "high-uptake plants" due to their elevated metal(loid) accumulation.

PLS-R models were applied to identify which soil parameters

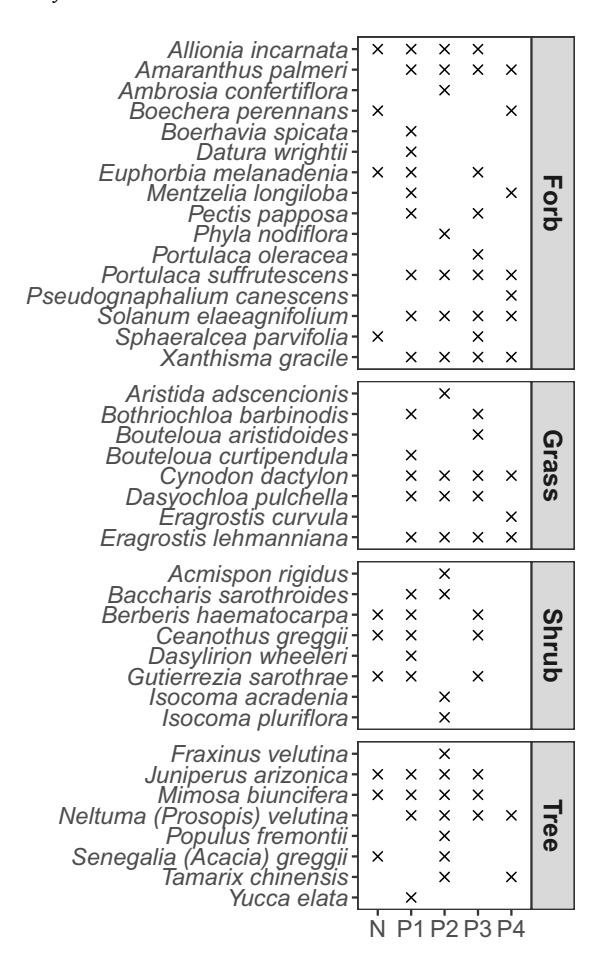


Fig. 4. Species identified in the study area organized by plant form (forbs, grasses, shrubs, trees). x indicates species presence in a study plot (P1, P2, P3, P4) at the tailing facility and at the undisturbed natural site (N).

influenced concentrations of Cu, Se, Re, Zn, Mn, Fe, P, S in plant leaves. Among these, only the Cu model showed moderate model robustness and predictive ability, with a cross-validation criterion of $Q^2 = 0.33$, exceeding the recommended threshold of 0.15 (Hair et al., 2021). In contrast, the models for the remaining elements exhibited very low predictive power ($Q^2 < 0.1$; see Supplementary Materials: PLS-R output information). Several soil parameters had significant standardized coefficients in the Cu model, with pH showing the strongest negative influence on Cu concentrations and total Mo showing the strongest positive effect. Other significant negative predictors included extractable Ca, Mn, and Mg, while extractable Cu and S were significant positive predictors. In addition, plot P4 had a strong positive association with Cu concentrations in plants, whereas other plots had marginal explanatory effects (Tables S5 and S6). Overall, these results suggest that both soil chemistry and local plot conditions can strongly influence metal(loid) uptake, highlighting the importance of considering spatial heterogeneity and soil-specific constraints when selecting plant species for mine reclamation strategies.

3.3. Differences in vegetation structure and coverage between plots

Our remote sensing-derived metrics of vegetation structure were in agreement with the field observations in terms of the vegetation distribution at the tailings pond plots and the natural site. Plot P3 had the highest percentage of vegetation cover (18 % shrubs and trees) and the highest median vegetation height (\sim 0.5 m) among all plots at the tailings pond. Accordingly, it also had the lowest proportion of bare soil (0.4 %), whereas plot P4 had the highest (96 %). Plot P2 contained the

tallest but sparsely distributed individual trees (maximum height). In addition, this plot had the greatest tree-species richness (Fig. 4). The natural plot had almost three times greater shrub and tree cover (52 %) than P3 and also more bare soil (10 %) than any other plot except P4. The natural plot also had the highest mean vegetation height overall. These patterns are likely due to the denser distribution of shrubs and trees and the low proportion of grasses and forbs (38 % at the natural plot compared to 81 % at P1 and P3 and 90 % at P2; Table 3, Figs. S3, S4).

3.4. (Hyper)accumulation of elements by high-uptake plants at the revegetated tailings pond

Elemental concentrations of Cu, Se, Re, Zn, Mn, Fe, P, and S in shoots of "high-uptake plants" across all tailings plots were compared to the respective thresholds for maximum optimal concentrations in plant tissues and for hyperaccumulation (Fig. S5). For Cu, Se, and Re, the maximum optimal thresholds were 30 mg kg⁻¹, 2 mg kg⁻¹, and 5 mg kg⁻¹, respectively (Kabata-Pendias, 2011; Novo et al., 2018), whereas the global hyperaccumulation thresholds were 300 mg kg⁻¹, 100 mg kg⁻¹, and 100 mg kg⁻¹, respectively (Reeves et al., 2017; Tabasi et al., 2018). Among the analyzed elements, Cu was the only one to reach the hyperaccumulation level, with two species (Pseudognaphalium canescens (DC.) W.A. Weber and Xanthisma gracile (Nutt.) D.R. Morgan & R.L. Hartm.) exceeding the 300 mg kg⁻¹ threshold at plot P4. Additionally, eight species had Cu concentrations above the maximum optimal threshold, classifying them as Cu accumulators. Se accumulation was observed in most high-uptake plants, with eight species exceeding the maximum optimal concentration, and one species (Isocoma acradenia Greene) approaching the global hyperaccumulation threshold. Similarly, five species were identified as Re accumulators, with one species (S. greggii) nearing the global hyperaccumulation threshold and four exceeding the maximum optimal threshold.

3.5. Reference elemental composition of "high-uptake" species from natural ecosystems

Herbarium scanning with the pXRF revealed intra-specific variability in the elemental composition of "high-uptake" species and indicated population-driven patterns in plants growing at the tailings pond (Fig. 6, Table S7). For Cu, most specimens displayed optimal concentrations except for Mentzelia longiloba J. Darl., I. acradenia, and Isocoma pluriflora Greene, several specimens of which approached or exceeded concentrations recorded at the tailings pond. At least one herbarium specimen per high uptake species confirmed the Se accumulation, with several specimens of I. acradenia, Tamarix chinensis Lour., Senegalia greggii and M. longiloba surpassing the average Se concentrations measured in the field. Rhenium concentrations remained within optimal ranges, except for slightly elevated concentrations in a few specimens of S. greggii, I. acradenia, M. longiloba, and I. pluriflora. In most herbarium specimens, Zn, Mn, P, and Fe concentrations were comparable to those observed at the tailings pond, with the exception of Pseudognaphalium canescens, which exhibited higher Mn and Fe concentrations across multiple locations. Sulfur concentrations were substantially higher in B. perennans, T. chinensis, A. incarnata, and I. pluriflora at either the natural site, the tailings pond, or both, compared to their conspecific herbarium specimens.

4. Discussion

Whereas phytoremediation remains challenging in dryland settings due to the multitude of combined abiotic stresses, the chosen study site presented us with a rare opportunity to study a well-established plant community many decades after the initial tailing revegetation. The spatial heterogeneity and local diversity of this plant community were particularly interesting with a view of the past and future

Total concentrations (mean \pm SD) of elements in the leaves of plants species found at both the tailings pond and the neighboring natural site. For the tailings pond plots, the average value represents all replicates of a given species across all plots where the species was present.

	•	•															
Species name	Site	$\rm Cu \\ mg \ kg^{-1}$		${\rm Se} \\ {\rm mg \ kg}^{-1}$		${\rm Re} \\ {\rm mg} \ {\rm kg}^{-1}$		$_{\rm mg~kg^{-1}}^{\rm Zn}$		$\rm Mn \\ \rm mg \; kg^{-1}$		$_{\rm mgkg^{-1}}$		$^{\rm p}_{\rm mg~kg^{-1}}$		$_{\rm mg~kg^{-1}}^{\rm S}$	
Allionia incarnata	NATURAL TAIL INGS	30 ± 7 80 ± 43	*	11 ± 3	* *	6.8 ± 2.7	su	19 ± 3	su	46 ± 13	su	1056 ± 671	su	2192 ± 54	su	$97,691 \pm 25,416$	*
Berberis haematocarpa	NATURAL TAILINGS	$8.2 \pm 1.2 \\ 5.4 \pm 1.4$	*	0.4 ± 0.1 1.2 ± 0.9	*	0.1 ± 0.1 0.5 ± 0.3	*	15 ± 10 15 ± 4 10 ± 3	ns	157 ± 65 18 ± 21	* *	1035 ± 1012 42 ± 5 26 ± 4	* *	1697 ± 303 1766 ± 936	us	$21,520 \pm 26,500$ 9257 ± 516 1650 ± 1921	*
Boechera perennans	NATURAL	17 ± 2 179 ± 88	* *	3.8 ± 1.0 4.2 ± 3.0	us	0.04 ± 0.01 0.9 ± 0.5	* *	16 ± 4 45 ± 7	*	56 ± 23 34 ± 13	su	121 ± 31 364 \pm 249	su	2172 ± 443 2970 ± 1984	us	$41,772 \pm 3358$ 66.112 ± 82.141	us
Ceanothus greggii	NATURAL	6.8 ± 1.0 15 ± 3	*	0.2 ± 0.1 1.9 ± 1.5	*	3.1 ± 2.5 1.5 ± 0.8	su		su	33 ± 8 44 ± 26	su	$54\pm7\\112\pm41$	* *	$1940 \pm 165 \\ 1267 \pm 304$	*	8149 ± 1071 9922 ± 10.080	us
Euphorbia melanadenia	NATURAL TAILINGS	$14\pm1\\36\pm23$	us	$0.9\pm0.2\\1.1\pm1.3$	us	$\begin{array}{c} 0.006 \pm 0.003 \\ 0.1 \pm 0.1 \end{array}$	*	$13\pm1 \\ 23\pm10$	*	49 ± 19 30 ± 14	us	$111\pm14\\351\pm342$	us	$2413 \pm 564 \\ 2080 \pm 517$	us	8376 ± 1244 9676 ± 8981	su
Gutierrezia sarothrae	NATURAL TAILINGS	$12\pm2.5\\30\pm9.5$	*	$0.9\pm0.3\\1.3\pm0.9$	ns	0.04 ± 0.01 1.3 ± 1.1	* *	$\begin{array}{c} 28 \pm 4 \\ 33 \pm 21 \end{array}$	ns	$42\pm17\\39\pm25$	us	51 ± 4 115 ± 81	*	$1945 \pm 171 \\ 2913 \pm 1449$	us	$12,456 \pm 2176 \\ 6213 \pm 12,609$	su
Juniperus arizonica	NATURAL TAILINGS	7.3 ± 2.1 12 ± 4.6	us	$0.5\pm0.2\\0.7\pm0.3$	ns	$0.3 \pm 0.2 \\ 0.2 \pm 0.1$	su	$\begin{array}{c} 8 \pm 2 \\ 14 \pm 4 \end{array}$	*	$25\pm19\\43\pm31$	us	57 ± 15 70 ± 31	us	1143 ± 159 1793 ± 429	*	6705 ± 477 7153 ± 6920	su
Mimosa biuncifera	NATURAL TAILINGS	$\begin{array}{c} 9\pm1 \\ 45\pm15 \end{array}$	* *	$\begin{array}{c} 0.9 \pm 0.5 \\ 3.9 \pm 2.6 \end{array}$	*	0.03 ± 0.01 4.9 ± 2.2	*	$19\pm2\\14\pm6$	us	121 ± 6 59 ± 25	*	$69\pm2\\117\pm62$	*	$2293 \pm 133 \\ 1915 \pm 924$	us	$18,351 \pm 386 \\ 8982 \pm 8044$	su
Senegalia greggii	NATURAL TAILINGS	$10\pm1\\82\pm1$	*	$2.0\pm0.4\\11\pm8$	us	$2.5\pm1.4\\64\pm31$	* *	$\begin{array}{c} 21 \pm 5 \\ 21 \pm 4 \end{array}$	us	$23\pm 6\\138\pm 17$	* * *	$55\pm4\\106\pm11$	* * *	$2675 \pm 485 \\ 1050 \pm 73$	*	$16,\!100\pm710\\2191\pm319$	* * *
Sphaeralcea parvifolia	NATURAL TAILINGS	$12\pm1\\59\pm13$	*	$0.6\pm0.1\\0.9\pm0.7$	su	$\begin{array}{c} 0.7\pm1.1 \\ 0.3\pm0.1 \end{array}$	su	12 ± 6 42 ± 21	su	$56\pm20\\38\pm18$	su	$83\pm9\\338\pm79$	* *	$1949 \pm 506 \\ 3093 \pm 825$	us	$24,484 \pm 14,586 \\ 6127 \pm 2542$	*
																- 1	

 $\begin{array}{l} \text{ns} - \text{non-significant.} \\ * & p \leq 0.05. \\ ** & p \leq 0.01. \\ *** & p \leq 0.01. \end{array}$

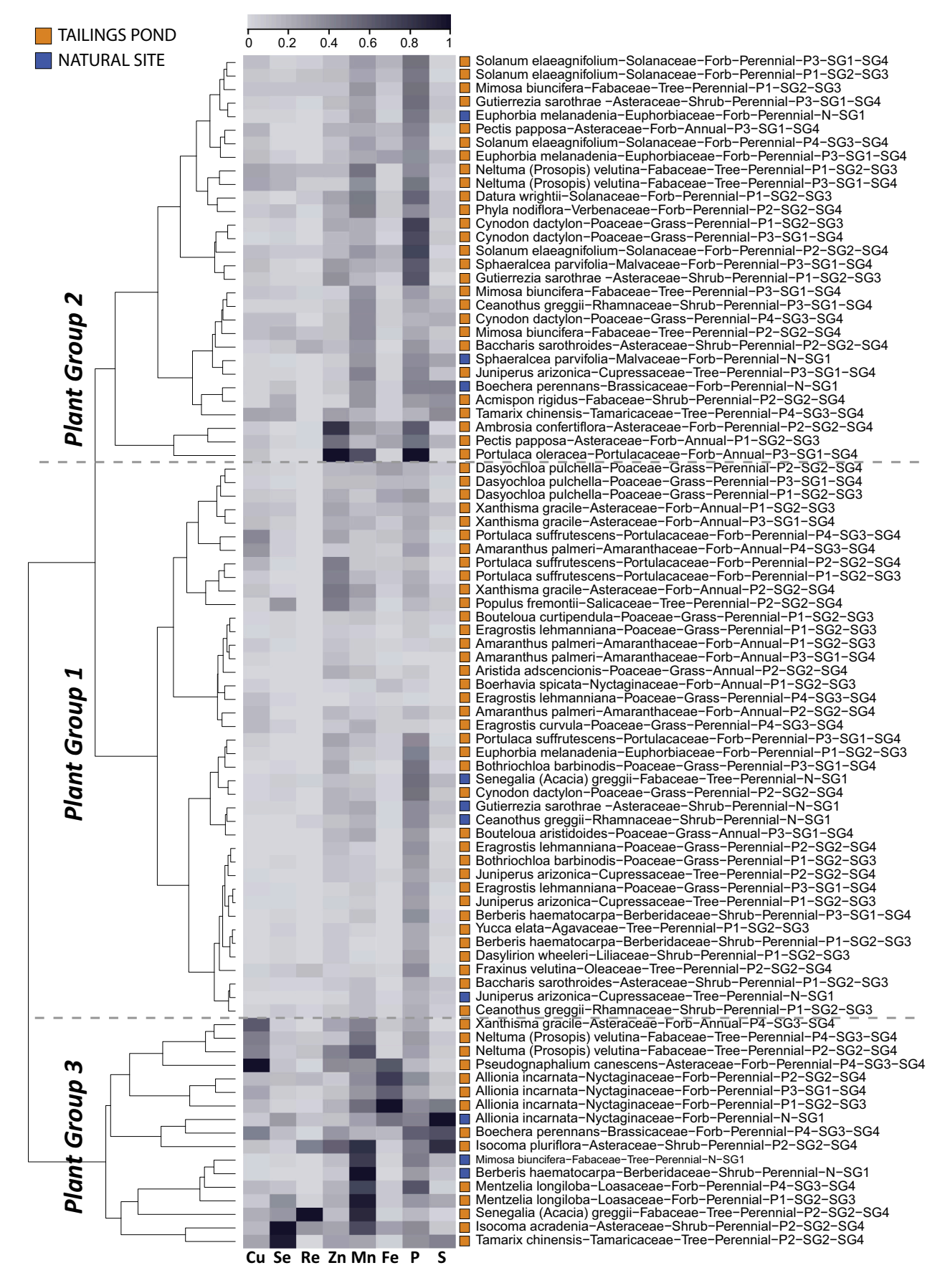
phytomanagement of mine legacy sites. Phytostabilization has to date been the go-to approach in drylands and our survey detected a number of metal-excluding species that appear suitable for the immobilization of contaminants in the substrate. At the same time, we found several key species with metal-accumulation capabilities at the study site, some of which have previously been considered excluders. Because plant metal accumulation has remained understudied in drylands and because of a worldwide push towards secondary metal extraction from previously disposed mine waste, we focus parts of our discussion below on these metal accumulators. While we do not anticipate phytoextraction to challenge phytostabilization as the primary phytoremediation approach in drylands, much can be learned from these plants regarding their internal processes related to metal tolerance, as well as their underexplored potential for application in phytomining. In the following, we elaborate on the drivers of the present vegetation structure, the substrate properties that impact plant metal accumulation, the surprising levels of Cu, Se, and Re accumulation in certain key species, as well as our novel herbarium-based approach to screen for these accumulation traits across the species' larger distribution range in the U.S. Southwest.

4.1. Revegetation success remains spatially heterogeneous after 60+ years

Our results revealed substantial spatial heterogeneity in revegetation success across the tailings pond, with marked differences in vegetation structure, surface soil cap thickness, and substrate biochemistry. While most of the pond supported vegetation cover to varying degrees, two regions stood out: one represented by plot P3 that showed clear signs of well-advancing ecosystem recovery; and the other represented by plot P4 where the vegetation was extremely sparse compared to the off-tailing natural reference plot.

The area represented by plot P3 most closely resembled the neighboring undisturbed site in terms of top soil characteristics and vegetation structure. The two areas also shared the highest number of overlapping species compared to other plots, underscoring that the plant community at P3 is on a trajectory towards near-natural conditions. Remote sensing-derived metrics of vegetation structure aligned closely with traditional field observations and confirmed P3's advanced vegetative status along with the lowest proportion of bare soil across the tailings pond. The favorable conditions at P3 are likely driven by multiple interrelated factors. Firstly, the surface soil layer was considerably thicker (~30 cm) compared to other parts of the tailings pond and also to the initial capping layer applied during reclamation in the 1960s (~15 cm). This difference likely reflects a combination of uneven initial capping application and the long-term buildup of organic matter and soil development over 60+ years of vegetation establishment. Secondly, organic matter content exceeded the ranges typically found in Arizona soils (0.1-1.0 %) (Fuller and Wallace, 1965), likely enhancing nutrient cycling, water holding capacity, soil aggregation, as well as microbial diversity (Brevik et al., 2015; Singh et al., 2023). Correspondingly, concentrations of key nutrients (extractable K, Ca, Mn, and total Ni) and microbial biomass were highest in the surface layer of P3, creating a favorable substrate for plant establishment (Murawska-Wlodarczyk et al., 2025). Additionally, organic matter can mitigate plant metal(loid) stress (Caporale and Violante, 2015), counterbalancing substrate toxicity and further reinforcing long-term ecosystem recovery. Lastly, the moderately alkaline pH at P3 likely contributed to reduced metal (loid) bioavailability, as reflected by relatively low fractions of extractable Cu compared to other plots.

Despite the relative revegetation success at P3, the tree and shrub cover remained nearly three times less than at the natural site. Mean vegetation height was also reduced, largely due to the twice higher grass-fraction compared to the shrub- and tree-dominated community that prevails off-tailing. This disparity raises an important question: does P3 represent the best revegetation outcome achievable under the region's semi-arid climate and the challenging substrate conditions of



(caption on next page)

Fig. 5. Concentrations of Cu, Se, Re, Zn, Mn, Fe, P, S in plant leaves from the revegetated tailings pond and the neighboring natural site. Each column of the heatmap represents one element; each row represents a species name and its associated family, form (grass, forb, shrub, tree), life cycle (annual, perennial), plot (P1, P2, P3, P4, N), and substrate group (SG1, SG2, SG3, SG4). The first substrate group refer to surface layer, and the second one (if present), refers to tailings layer in the soil. Elemental concentrations were averaged for each plant species within the sampling location (plots and natural site) where they occurred. The values were normalized using min-max scaling to enable comparison across elements, according to the formula: $x' = (x - x_{min}) / (x_{max} - x_{min})$, where x is observed cocnentration, x_{min} and x_{max} are the minimum and maximum concentrations for a given element, and x' is the normalized value ranging from 0 to 1. Hierarchical clustering was performed to identify groups with similar elemental composition pattern. Colored squares on the right side of the heatmap indicate the occurance of the species at the tailings pond site (orange) and the natural site (blue).

Table 3
Classification coverage percentages and zonal statistics for height distribution across four plots at the tailings pond (P1:P4) and the natural plot.

Area type	Total area (m ²)	Vegetation (%)	Vegetated-soil (%)	Bare soil (%)	Vegetation	n height (m)		
					Min	Max	Mean \pm SD	Median
Plot 1	11,700	17	81	2	0.02	3.0	0.36 ± 0.50	0.13
Plot 2	11,700	9	90	1	0.02	7.1	0.41 ± 0.77	0.14
Plot 3	11,700	18	81	0.4	0.002	3.5	0.49 ± 0.68	0.15
Plot 4	1293	0.9	3	96	0.03	2.0	0.12 ± 0.13	0.09
Natural plot	11,700	52	38	10	0.02	6.7	1.5 ± 1.0	0.8

legacy tailings, even after six decades of successful revegetation? In this context, we note that the observed difference in vegetation structure likely reflects distinct successional stages: the tailings pond is dominated by grasses and early-successional species, indicating an earlier stage of ecosystem recovery. By contrast, the natural site with its shrub and tree dominance reflects a later successional plant community that is structurally more complex. Whether the P3 vegetation will eventually transition towards this complex type of community or remain locked in a grass-dominated state will likely depend on further changes in soil properties and microclimate. Answering our question will thus require continued long-term monitoring, comparable observations at other reclaimed and un-reclaimed mine tailing facilities, and possibly experimental interventions to accelerate plant community succession.

In stark contrast to P3, plot P4 covered only a unique and very small portion of the tailings pond that was almost completely devoid of vegetation, apart from sparse individuals restricted to isolated patches. This plot had an extremely thin or even absent surface soil layer, and remote sensing confirmed 96 % bare soil cover – the highest of all plots. In this context, we note the challenge of distinguishing between barren soil patches and dry grass litter in optical remote sensing data (see the additional discussion in the Supplementary Materials). Such poor soil cover suggests inadequate capping during the original reclamation effort and subsequent wind or water erosion that likely removed seeds and organic matter, exposing harsh tailings. This substrate degradation led to the formation of a localized metal(loid) hotspot and hostile edaphic conditions that impeded vegetation establishment. Indeed, the surface layer of P4's substrate had elevated metal(loid) concentrations, often exceeding those found in the deeper tailings layer. This could be the result of vertical diffusion or hydraulic upward movement of metal(loid) s from tailings to the surface soil (Amnai et al., 2021).

These unmistakable differences between the areas represented by P3 and P4 underscore that heterogeneity in surface soil thickness and biochemical properties can determine the success or failure of revegetation efforts at legacy mine sites even decades after reclamation. This highlights the importance of careful capping techniques, ongoing soil development and vegetation progression, and continuous long-term monitoring to ensure ecosystem sustainability. In practice, our findings suggest that applying a relatively thick capping layer (>30 cm) may help reduce erosion and topsoil loss. At the same time, thick caps will limit the upward movement of metal(loid)s from the underlying tailings to the surface and thereby reduce associated hazards for dust emissions and food chains.

4.2. Substrate properties, not species identity, drive patterns of plant metal (loid) accumulation

Differences in elemental composition of plants at the revegetated tailings pond closely mirrored substrate heterogeneity, highlighting the dominant role of surface soil properties in shaping metal(loid) accumulation patterns and vegetation chemistry. While such a relationship might be expected for shallow-rooted species such as grasses and annuals, our findings indicate that this pattern prevailed across the entire vegetation community at the study site regardless of plant functional type. The apparent absence of root penetration into the underlying tailings, evidenced by the lack of organic fragments in deeper layers, further supports our conclusion that surface substrate conditions exert stronger control over plant chemistry than species-specific traits or deeper substrate composition.

Although metal(loid) accumulation can vary with plant species and genotype, our data show that the chemical and physical properties of the surface substrate at specific plots consistently shaped uptake patterns across most taxa. This was reflected by the broader grouping of species based on their elemental profiles. Plant Group 1, which was dominated by Poaceae grasses and annuals, had the lowest concentrations of most elements and was mainly associated with the natural site and with surface soils at P3 (Substrate Group 1). Plant Group 2, a mix of functional types, showed intermediate elemental concentrations and also occurred predominantly in Substrate Group 1 plots. In contrast, Plant Group 3, which included many forbs but few grass and tree species (and notably no shrubs), was largely confined to P4 (Substrate Group 3). This group displayed the highest relative uptake of multiple elements, particularly Cu and Mn. Ten species from Plant Group 3, all occurring within the revegetated tailings pond, were identified as "high-uptake plants" due to their consistently elevated metal(loid) concentrations. This suggests that substrate characteristics exerted a stronger influence than plant functional type or taxonomic identity in determining metal (loid) accumulation.

The most notable example of plant metal(loid) uptake was that of Cu accumulation in plot P4 (Substrate Group 3), where a markedly thinner – or absent – surface soil layer corresponded with elevated foliar concentrations across nearly all species. In some cases, plants shifted from optimal Cu levels at other plots (P1–P3) to Cu accumulator status in P4. The only exception was *Solanum elaeagnifolium* Cav., which maintained stable and relatively low Cu concentrations regardless of location. Several substrate-driven factors likely contributed to the enhanced metal(loid) accumulation pattern in plants from P4, including: i) the relatively low mean pH of Substrate Group 3 that likely increased extractable Cu and facilitated plant uptake, which is consistent with

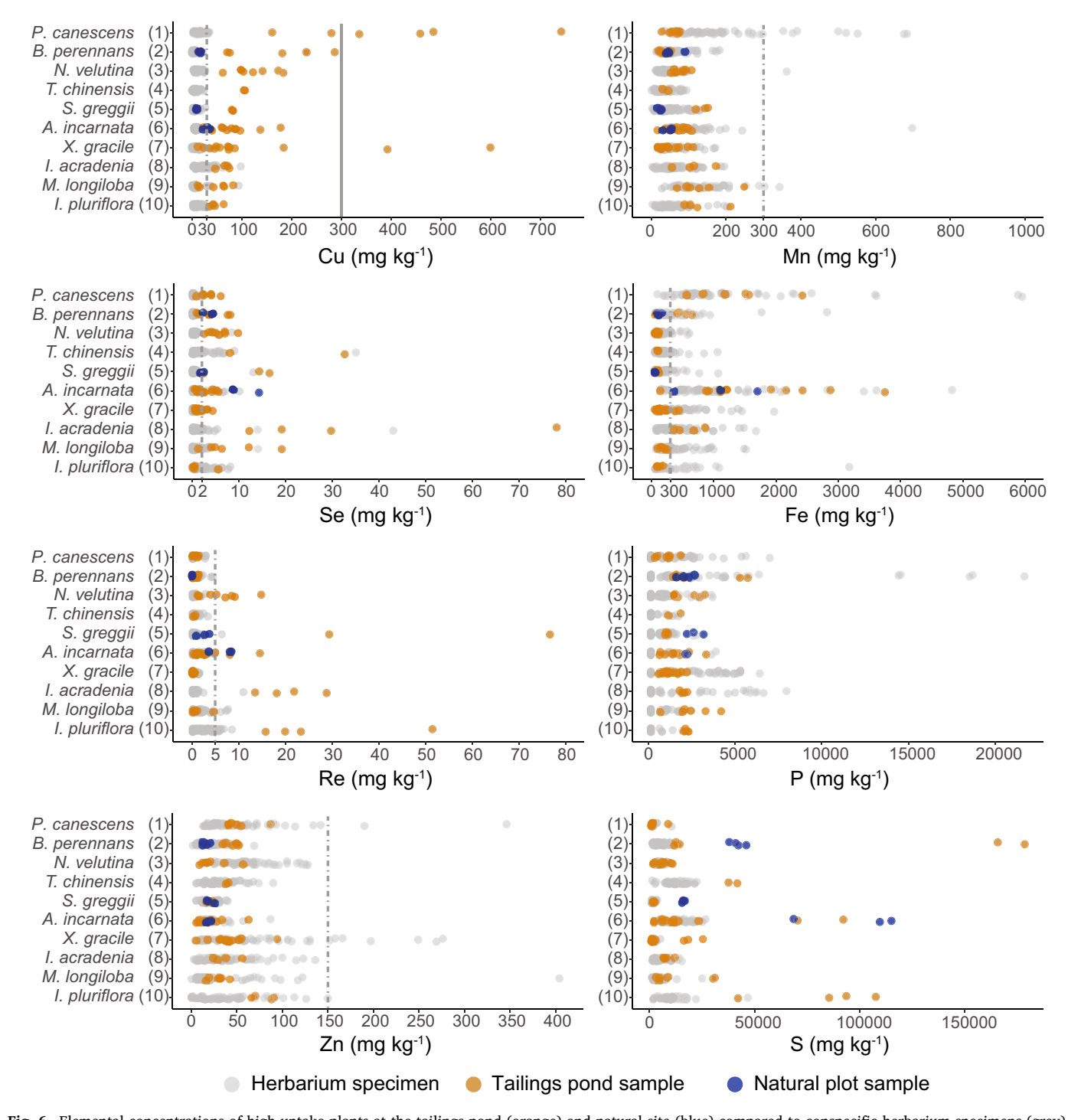


Fig. 6. Elemental concentrations of high-uptake plants at the tailings pond (orange) and natural site (blue) compared to conspecific herbarium specimens (grey). Each grey dot represents the mean leaf concentration of a herbarium specimen representing an independent location within the species distribution captured by the herbaria collection. A light-grey solid line represents the hyperaccumulation threshold and the short-dashed line represents a maximum optimal level in plant for a given element.

known effects of pH on metal(loid) bioavailability (Caporale and Violante, 2015); ii) elevated extractable S concentrations, which has previously been linked to increased metal(loid) accumulation (Nkrumah et al., 2019); iii) elevated total Mo concentrations, potentially promoting Cu uptake; and iv) low concentrations of extractable Mn, Ca and Mg compared to both typical soil values for Arizona (Chesworth et al., 2008; Martin, 1940) and to their corresponding levels in other plots. Such nutrient imbalances may indirectly promote Cu accumulation through various physiological pathways. One such example is Mg deficiency,

which has been shown to stimulate Cd transport in both apoplastic and symplastic regions of plants (Borisev et al., 2016). This movement happens potentially via non-specific cation transporters, which may also facilitate Cu uptake (Burzyński et al., 2005).

Other elements also exhibited distinct substrate associations. Selenium uptake was linked primarily to Substrate Group 2, with some species shifting between accumulation and exclusion strategies depending on plot conditions. Rhenium uptake was also associated with Substrate Group 2, despite higher Re concentration in Substrate Group

3. This contrasts with previous studies that generally reported a positive relationship between soil and plant Re concentrations (Novo et al., 2018). We thus expect factors other than those assessed in this study to at least partly influence the plant uptake and accumulation of certain metal(loid)s at this semi-arid revegetated tailings pond. In this regard, we recommend that future work should also investigate soil texture, moisture content, microbial community composition, and plant-microbial interactions as co-determinants of metal(loid) accumulation. Studies testing these relationships experimentally using controlled trials with representative species and substrates could prove particularly valuable for refining substrate management strategies and thus for improving revegetation outcomes in challenging post-mining landscapes.

4.3. Evidence for new Cu, Se, and Re (hyper)accumulators from this field study

Our field survey identified several species with elevated metal(loid) accumulation, including two that exhibited Cu hyperaccumulaton in their foliage. *Pseudognaphalium canescens* and *Xanthisma gracile* had the highest foliar Cu accumulation among all sampled species and exceeded the global hyperaccumulation threshold of 300 mg kg $^{-1}$ (Reeves et al., 2017) in individuals from plot P4. To our knowledge, this is the first evidence of Cu hyperaccumulation in these species. Whereas other *Pseudognaphalium* species have been reported to accumulate Cu and Zn at mine tailings (Santos et al., 2017), our findings expand the list of potential hyperaccumulators in arid environments. This is an important outcome of our plant survey given the rarity of Cu hyperaccumulators in natural systems (Lange et al., 2017; Widmer and Norgrove, 2023) where most species act as Cu excluders and concentrations in leaves rarely exceed 100 mg kg $^{-1}$.

In addition to the two hyperaccumulators, our study identified several other species that accumulated >100 mg Cu kg $^{-1}$ in their foliage, a concentration that is often considered the minimum for economically viable Cu phytoextraction (Mattiello et al., 2023). Such elevated Cu levels also lend themselves for the valorization of plant biomass, for example in ecocatalysis (Cybulska et al., 2022). One notable species is Boechera perennans that occurred in a small patch on plot P4 and accumulated >170 mg Cu kg⁻¹. Interestingly, we found *B. perennans* also at the natural site where - despite Cu-enriched soils - the species maintained low Cu concentrations (Table 2). This suggests strong intraspecific variability in Cu uptake. Although metal(loid) accumulation in Boechera is poorly understood, its evolutionary history is characterized by frequent polyploidy and apomixis (Windham et al., 2022). The genus is also genetically close to the Zn/Cd-hyperaccumulating genus Arabidopsis (Babst-Kostecka et al., 2018), which points to high adaptive potential to metal(loid)-contaminated sites. Boechera's higher thermotolerance and photosystem II protection under heat stress compared to the model species A. thaliana (Halter et al., 2017) further adds to its potential for arid-land remediation research.

Another species of interest is *Neltuma velutina* (Wooton) Britton & Rose (Velvet mesquite; syn. *Prosopis velutina* Wooton), which is often considered an aggressive native invader of grass-dominated systems. Our observed values of Cu accumulation >100 mg kg $^{-1}$ align with earlier reports of 200 mg kg $^{-1}$ in foliage (Santos et al., 2017). Other members of this genus are known to accumulate multiple metal(loid)s (Ramirez et al., 2019), indicating genus-wide tolerance to metal(loid) exposure. Similarly, we found that *Tamarix chinensis*, a halophytic invasive species known for efficient salt excretion, also exceeded >100 mg Cu kg $^{-1}$. Although generally considered a metal(loid) excluder, its frequent occurrence at contaminated sites highlights broad metal(loid) tolerance and thus potential for phytoremediation (Bu-Olayan and Thomas, 2013), and – as suggested by our results – Cu phytoextraction.

Further species with elevated metal(loid) uptake included *Senegalia greggii* (catclaw acacia). Interestingly, *S. greggii* showed a distinctive elemental composition profile with both high Re accumulation (>60 mg

 kg^{-1}) and moderate Cu accumulation (~80 mg kg⁻¹). At the natural site where soil Re levels were approximately three times lower than at the tailings site, *S. greggi* still accumulated ~10 mg Re kg⁻¹. Although these values remained below the formal hyperaccumulation threshold for Re (100 mg kg⁻¹; (Tabasi et al., 2018)), they greatly exceeded typical plant concentrations (<5 mg kg⁻¹; (Novo et al., 2018)). Considering the high market value of Re and the potential feasibility of Re phytomining, *S. greggii* represents a promising new candidate to be studied alongside other acacia species that are known to hyperaccumulate Re (Bozhkov et al., 2008).

Other noteworthy taxa included two species of *Isocoma* (*I. pluriflora* and *I. acradenia*) that showed moderate Cu (up to 65 mg kg $^{-1}$) and Re (up to 30 mg kg $^{-1}$) accumulation. *I. acradenia* also surpassed one-third of the Se hyperaccumulation threshold, suggesting (hyper)accumulation potential in semi-arid environments. Several *Allionia incarnata* plants exhibited moderate Cu and Re accumulation, which may partially result from foliar dust deposition facilitated by sticky trichomes. Yet, the observed foliar Cu concentrations exceeded those found in the surface soils and it is thus unlikely that dust deposition alone would explain the elevated Cu levels. Lastly, some individuals of *Mentzelia longiloba*, which is known to be adapted to disturbed arid soils and has previously been reported at mining sites (Schenk and Hufford, 2010), accumulated moderate Cu (\sim 60 mg kg $^{-1}$) and elevated Se (>10 mg kg $^{-1}$) concentrations. Hence, *M. longiloba* emerged as another species that may be explored for its metal(loid) accumulation potential.

Overall, our findings align with previous studies showing that Cu hyperaccumulation is often population-specific and strongly driven by the micro-environment (Lange et al., 2017; Mattiello et al., 2023). Many species tolerate high Cu concentrations in the substrate without hyperaccumulating it, making them suitable for phytostabilization. However, the exceptional Cu concentrations that we found in P. canescens and X. gracile exceeded the hyperaccumulation threshold and were well beyond the minimum economic benchmark (Widmer and Norgrove, 2023). This positions them as highly promising candidates for phytoextraction trials and for the sustainable remediation of Cucontaminated arid lands in general. In this respect, we note the comparatively low and short-lived biomass of desert and steppe plants, making biomass data (which we did not collect in this study) an essential part of a full economic evaluation. Future research should also quantify intra-specific variability in Cu accumulation for these taxa, evaluate their performance under controlled conditions, and assess their potential in breeding programs targeting more tolerant and efficient

4.4. pXRF scanning of herbarium collections uncovers inherent capacity for metal(loid) accumulation in high-uptake plants: a promising approach to advance phytomining

The fact that we observed highly substrate-specific elemental accumulation patterns in plants from the tailings pond points to environmental heterogeneity that can shape genetic diversity and drive local adaptation of metal(loid) accumulation traits (Babst-Kostecka et al., 2018). Such site-specific adaptation can create substantial intra-specific variability in metal(loid) accumulation, which challenges conclusions regarding the overall phytomining potential of candidate species based on observations from a single site. We overcame this challenge by developing a non-standard approach to place our site observations in a broader ecological context by pXRF scanning of large numbers of herbarium specimens from "high-uptake" species identified in the field. Conventional pXRF herbarium scanning typically targets a single specimen per species and is followed by field surveys to investigate promising species in their native environments (Abubakari et al., 2021). Doing so risks overlooking potential hyperaccumulators when an insufficient number of populations is analyzed and specimens from anthropogenically modified locations are not included. Our study now demonstrates that by reversing this process, i.e., by first identifying candidate species at metalliferous sites before testing many herbarium counterparts from across their distribution range, we can better discern species-wide from population-specific accumulation patterns. Importantly, these specimens were collected from natural (presumably) uncontaminated environments, meaning the plants were unlikely to have experienced strong selection for elevated metal(loid) uptake. Regardless, herbarium specimens of all ten "high-uptake" species from various locations often exceeded maximum optimal concentrations for multiple elements, including Cu, Mn, Se, Fe, Re, and Zn in plant tissues, though none reached the respective hyperaccumulation thresholds. Notable examples included Cu accumulation >100 mg kg⁻¹ in *I. acradenia* from the Colorado River bank, the Grand Canyon National Park, and the Tonto National Forest, as well as in M. longiloba collected in the vicinity of a Cu mining facility. The latter location could experience either natural soil Cu enrichment, dust deposition, or colonization by plants from neighboring mining-impacted land with possible pre-adaptation. Rhenium accumulation was also widespread and populationdependent, with S. greggi, I. acradenia, I. pluriflora, and M. longiloba speciments often situated above the maximum optimal levels. Isocoma acradenia from a salt-precipitating Grand Canyon site exhibited the highest Se accumulation, followed by T. chinensis with the second highest Se uptake recorded in a specimen from a halophytic habitat. This suggests that saline soil conditions may favor Se uptake.

As these elevated metal(loid) concentrations occurred in plants that likely grew in low-metal(loid) soils, our data suggest that the identified species possess an inherent capacity for above-optimal accumulation of various elements. This ability would facilitate the colonization of metalliferous sites where the same traits could be expressed more strongly. However, the elemental profiles of the native soils for these herbarium collections remain unknown, and the question of whether the observed uptake reflects phenotypic plasticity or heritable adaptation and species-wide features cannot yet be resolved. Given that adaptive evolution of metal(loid) tolerance and (hyper)accumulation traits can occur in both contaminated and uncontaminated environments (Babst-Kostecka et al., 2018), addressing this will require reciprocal transplant and controlled greenhouse experiments using populations from both high-uptake and baseline sites.

5. Conclusions

This study provides a comprehensive assessment of vegetation structure and richness, plant metal(loid) uptake, and ecosystem recovery at a fully revegetated tailings pond in a semi-arid part of the Southwestern U.S. By integrating remote sensing with field sampling and herbarium-based pXRF analysis, we present a novel framework for evaluating both revegetation success and the phytoremediation potential of the local flora. Remote sensing-derived metrics of vegetation structure aligned closely with traditional field plot observations, paving the way for the rapid detection of structural differences across heterogeneous tailings in support of targeted management and monitoring of degraded areas. Our work also expanded the pool of plant species with potential for phytoremediation in arid and semi-arid environments by identifying new (hyper)accumulators of Cu, Se, and Re. By creating a robust elemental baseline through the pXRF screening of conspecific herbarium specimens from multiple uncontaminated natural locations, we were able to evaluate species-level variation in metal(loid) accumulation traits among "high-uptake" species identified in the field. The frequent occurrence of element concentrations above maximum optimal levels in herbarium plants suggests that some populations possess an inherent capacity to colonize and persist on metalliferous substrates. However, the pronounced variability in metal(loid) uptake among populations indicates that these traits are often site- or ecotype-specific rather than universally expressed across a species. Together, these findings deepen our understanding of plant adaptation, metal(loid) accumulation, and ecosystem regeneration in reclaimed mine tailings. This multi-layered approach offers a robust framework to guide future revegetation efforts and to improve the sustainability of legacy mine sites in drylands.

Supplementary data to this article can be found online at https://doi.org/10.1016/j.scitotenv.2025.180705.

CRediT authorship contribution statement

Tomasz Włodarczyk: Writing – original draft, Visualization, Methodology, Investigation, Formal analysis, Data curation, Conceptualization. Flurin Babst: Writing – review & editing, Resources. Kamila Murawska-Włodarczyk: Writing – review & editing, Investigation. Owyn Stokes: Investigation. Andrew Salywon: Writing – review & editing, Resources. Willem J.D. van Leeuwen: Resources, Investigation. Cynthia Libantino Norton: Investigation. Shelby Rader: Investigation. Raina M. Maier: Writing – review & editing, Funding acquisition. Alicja Babst-Kostecka: Writing – review & editing, Supervision, Investigation, Funding acquisition, Conceptualization.

Declaration of Generative AI and AI-assisted technologies in the writing process

During the preparation of this work the authors used ChatGPT 4 in order to improve the readability of text and grammar. After using this tool/service, the authors reviewed and edited the content as needed and take full responsibility for the content of the published article.

Funding

This work was supported by the University of Arizona Center for Environmentally Sustainable Mining Industry-Academic Revegetation Research Cooperative, the University of Arizona School of Mining and Mineral Resources, LabEx DRIIHM, French programme 'Investissements d'Avenir' (ANR-11-LABX-0010), which is managed by the ANR and within the framework of the OHMi Pima County (2022–2023/4), Centre National de la Recherche Scientifique (CNRS) that funded graduate fellowship of the leading author, and the National Institute of Environmental and Health Sciences Superfund Research Program [grant number P42ES004940] at the University of Arizona.

Declaration of competing interest

The authors declare that they have no known competing financial interests or personal relationships that could have appeared to influence the work reported in this paper.

Acknowledgements

We thank George Ferguson (University of Arizona Herbarium) for assistance with plant identification and facilitating access to herbarium specimens for pXRF scanning. We also acknowledge Filip Pošćić for his support during the field campaign, Anika Svenson for her contribution in herbarium pXRF scanning, and Shreya Kolte for assistance with remote sensing data processing. We acknowledge the BIO5 Institute at the University of Arizona for providing laboratory infrastructure and research support.

Data availability

Summary plant and herbarium data are provided in the supplementary materials. Raw data and analysis codes are available upon request.

References

Abubakari, F., Nkrumah, P.N., Erskine, P.D., Brown, G.K., Fernando, D.R., Echevarria, G., et al., 2021. Manganese (hyper)accumulation within Australian Denhamia

- (Celastraceae): an assessment of the trait and manganese accumulation under controlled conditions. Plant Soil 463, 205–223.
- Álvarez-Rogel, J., Peñalver-Alcalá, A., Jiménez-Cárceles, F.J., Carmen Tercero, M., Nazaret González-Alcaraz, M., 2021. Evidence supporting the value of spontaneous vegetation for phytomanagement of soil ecosystem functions in abandoned metal (loid) mine tailings. Catena 201, 105191.
- Amnai, A., Radola, D., Choulet, F., Buatier, M., Gimbert, F., 2021. Impact of ancient iron smelting wastes on current soils: legacy contamination, environmental availability and fractionation of metals. Sci. Total Environ. 776, 145929.
- Archer, S.R., Predick, K.I., 2008. Climate change and ecosystems of the southwestern United States. Rangelands 30, 23–28.
- Babst-Kostecka, A., Schat, H., Saumitou-Laprade, P., Grodzińska, K., Bourceaux, A., Pauwels, M., et al., 2018. Evolutionary dynamics of quantitative variation in an adaptive trait at the regional scale: the case of zinc hyperaccumulation in *Arabidopsis halleri*. Mol. Ecol. 27, 3257–3273.
- Baker, A.J.M., 1981. Accumulators and excluders strategies in the response of plants to heavy metals. J. Plant Nutr. 3, 643–654.
- Baker, A.J., Ernst, W.H., van der Ent, A., Malaisse, F., Ginocchio, R., 2010. Metallophytes: the unique biological resource, its ecology and conservational status in Europe, central Africa and Latin America. In: Ecology of Industrial Pollution, pp. 7-40.
- Borisev, M., Pajevic, S., Nikolic, N., Orlovic, S., Zupunski, M., Pilipovic, A., et al., 2016. Magnesium and iron deficiencies alter Cd accumulation in *Salix viminalis* L. Int. J. Phytoremediation 18, 164–170.
- Bozhkov, O., Tzvetkova, C., Blagoeva, T., 2008. An approach to rhenium phytorecovery from soils and waters in ore dressing regions of Bulgaria. In: Proc. WSEAS Intl. Conf. on Waste Management, Water Pollution, Air Pollution, Indoor Climate, Corfu, Greece, pp. 262–265.
- Brevik, E.C., Cerdà, A., Mataix-Solera, J., Pereg, L., Quinton, J.N., Six, J., et al., 2015. The interdisciplinary nature of soil. Soil 1, 117–129.
- Bu-Olayan, A.H., Thomas, B.V., 2013. Assessment of the ultra-trace mercury levels in selected desert plants. Int. J. Environ. Sci. Technol. 11, 1413–1420.
- Burzyński, M., Migocka, M., Kłobus, G., 2005. Cu and Cd transport in cucumber (*Cucumis sativus* L.) root plasma membranes. Plant Sci. 168, 1609–1614.
- Caporale, A.G., Violante, A., 2015. Chemical processes affecting the mobility of heavy metals and metalloids in soil environments. Curr. Pollut. Rep. 2, 15–27.
- Chesworth, W., Spaargaren, O., Hadas, A., Groenevelt, P.H., Otero, X.L., Ferreira, T.O., et al., 2008. Trace elements. In: Chesworth, W. (Ed.), Encyclopedia of Soil Science. Springer, Dordrecht.
- Cybulska, P., Legrand, Y.-M., Babst-Kostecka, A., Diliberto, S., Leśniewicz, A., Oliviero, E., et al., 2022. Green and effective preparation of α-hydroxyphosphonates by ecocatalysis. Molecules 27.
- Feldman, A.F., Reed, S., Amaral, C., Babst-Kostecka, A., Babst, F., Biederman, J., et al., 2024. Adaptation and Response in Drylands (ARID): community insights for scoping a NASA Terrestrial Ecology field campaign in drylands. Earth's Future 12.
- Fuller, Wallace, H., 1965. Soil Organic Matter. The University of Arizona: CALS Publishing Archive.
- Hair Jr., J.F., Hult, G.T.M., Ringle, C.M., Sarstedt, M., Danks, N.P., Ray, S., 2021. Partial Least Squares Structural Equation Modeling (PLS-SEM) Using R: A Workbook. Springer Nature, Cham.
- Halter, G., Simonetti, N., Suguitan, C., Helm, K., Soroksky, J., Waters, E.R., 2017. Patterns of thermotolerance, chlorophyll fluorescence, and heat shock gene expression vary among four *Boechera* species and *Arabidopsis thaliana*. Botany 95, 9–27.
- Hard, H.R., Brusseau, M., Ramirez-Andreotta, M., 2019. Assessing the feasibility of using a closed landfill for agricultural graze land. Environ. Monit. Assess. 191, 458.
- Kabata-Pendias, A., 2011. Trace Elements in Soils and Plants. CRC Press, Boca Raton, Florida.
- Lange, B., van Der Ent, A., Baker, A.J.M., Echevarria, G., Mahy, G., Malaisse, F., et al., 2017. Copper and cobalt accumulation in plants: a critical assessment of the current state of knowledge. New Phytol. 213, 537–551.
- Lewis, J., Hoover, J., MacKenzie, D., 2017. Mining and environmental health disparities in Native American communities. Curr. Environ. Health Rep. 4, 130–141.
- Macdonald, S.E., Landhäusser, S.M., Skousen, J., Franklin, J., Frouz, J., Hall, S., et al., 2015. Forest restoration following surface mining disturbance: challenges and solutions. New For. 46, 703–732.
- Maiti, S.K., Ahirwal, J., 2019. Chapter 3 ecological restoration of coal mine degraded lands: topsoil management, pedogenesis, carbon sequestration, and mine pit

- limnology. In: Vimal Chandra Pandey, K.B. (Ed.), Phytomanagement of Polluted Sites. Elsevier, Elsevier, pp. 83–111.
- Martin, W.P., 1940. Distribution and Activity of Azotobacter in the Range and Cultivated Soils of Arizona. College of Agriculture, University of Arizona (Tucson, AZ).
- Mattiello, A., Novello, N., Cornu, J.-Y., Babst-Kostecka, A., Pošćić, F., 2023. Copper accumulation in five weed species commonly found in the understory vegetation of Mediterranean vineyards. Environ. Pollut. 329, 121675.
- Mendez, M.O., Maier, R.M., 2008. Phytostabilization of mine tailings in arid and semiarid environments - an emerging remediation technology. Environ. Health Perspect. 116, 278–283.
- Murawska-Wlodarczyk, K., Kushwaha, P., Stokes, O., Rasmussen, C., Neilson, J.W., Maier, R.M., Babst-Kostecka, A., 2025. Depth-dependent heterogeneity in topsoil stockpiles influences plant-microbe interactions and revegetation success in arid mine reclamation. Sci. Total Environ. 1003, 180673.
- Nkrumah, P.N., Tisserand, R., Chaney, R.L., Baker, A.J.M., Morel, J.L., Goudon, R., et al., 2019. The first tropical 'metal farm': some perspectives from field and pot experiments. J. Geochem. Explor. 198, 114–122.
- Novo, L.A.B., Silva, E.F., Pereira, A., Casanova, A., Gonzalez, L., 2018. The effects of rhenium accumulation on Indian mustard. Environ. Sci. Pollut. Res. 25, 21243–21250.
- Peterson, R.A., 2021. Finding optimal normalizing transformations via best Normalize. R J. 13.
- Raj, A.N., Sharad, Bargali, 2023. Eco-restoration of degraded forest ecosystems for sustainable development. Land Environ. Manag. For. 273–296.
- Ramirez, V., Baez, A., Lopez, P., Bustillos, R., Villalobos, M.A., Carreno, R., et al., 2019. Chromium hyper-tolerant *Bacillus* sp. MH778713 assists phytoremediation of heavy metals by mesquite trees (*Prosopis laevigata*). Front. Microbiol. 10, 1833.
- Reeves, R.D., Baker, A.J., Jaffré, T., Erskine, P.D., Echevarria, G., van der Ent, A., 2017.
 A global database for plants that hyperaccumulate metal and metalloid trace elements. New Phytol. 218, 407–411.
- Roy, P.P., Roy, K., 2008. On some aspects of variable selection for partial least squares regression models. QSAR Comb. Sci. 27, 302–313.
- Rylott, E.L., Ent, A., 2025. Harnessing hyperaccumulator plants to recover technologycritical metals: where are we at? New Phytol. 246, 859–866.
- Santos, A.E., Cruz-Ortega, R., Meza-Figueroa, D., Romero, F.M., Sanchez-Escalante, J.J., Maier, R.M., et al., 2017. Plants from the abandoned Nacozari mine tailings: evaluation of their phytostabilization potential. PeerJ 5, e3280.
- Schenk, J.J., Hufford, L., 2010. Taxonomic novelties from Western North America in Mentzelia section Bartonia (Loasaceae). Madroño 57, 246–260.
- Singh, A.K., Zhu, X., Chen, C., Yang, B., Pandey, V.C., Liu, W., et al., 2023. Investigating the recovery in ecosystem functions and multifunctionality after 10 years of natural revegetation on fly ash technosol. Sci. Total Environ. 875, 162598.
- Stegink, T.G., Rader, S.T., 2024. Lead translocation and isotopic fractionation after uptake by *Brassica juncea* (Brown Mustard). ACS Earth Space Chem.8(11) 2187–2197.
- Sun, H., Zhang, J., Wang, R., Li, Z., Sun, S., Qin, G., et al., 2021. Effects of vegetation restoration on soil enzyme activity in copper and coal mining areas. Environ. Manag. 68, 366–376
- Tabasi, S., Hassani, H., Azadmehr, A.R., 2018. Field study on Re and heavy metal phytoextraction and phytomining potentials by native plant species growing at Sarcheshmeh copper mine tailings, SE Iran. J. Min. Environ. 9, 183–194.
- Tay, S.L., Scott, J.M., Craw, D., 2021. Natural rehabilitation of arsenic-rich historical tailings at the Alexander mine, Reefton, New Zealand. N. Z. J. Geol. Geophys. 64, 558–569.
- Towett, E.K., Shepherd, K.D., Lee Drake, B., 2016. Plant elemental composition and portable X-ray fluorescence (pXRF) spectroscopy: quantification under different analytical parameters. X-Ray Spectrom. 45, 117–124.
- United States National Weather Service. NOWData NOAA Online Weather Data, n.d. USEPA, 2006. In: Agency USEP (Ed.), Data Quality Assessment: Statistical Methods for
- USEPA, 2006. In: Agency USEP (Ed.), Data Quality Assessment: Statistical Methods for Practitioners QA/G-9S. Environmental Protection Agency.USGS, 2024. In: Center NMI (Ed.), Mineral Commodity Summaries 2024: U.S. Summary.
- USGS, 2024. In: Center NMI (Ed.), Mineral Commonity Summaries 2024: U.S. Summary. Widmer, J., Norgrove, L., 2023. Identifying candidates for the phytoremediation of copper in viticultural soils: a systematic review. Environ. Res. 216, 114518.
- Windham, M.D., Pryer, K.M., Allphin, L., 2022. An overview of New Mexican Boechera (Brassicaceae) including three new species and thirteen new nomenclatural combinations. J. Bot. Res. Inst. Texa 16, 9–24.